

CurvFed: Curvature-Aligned Federated Learning for Fairness without Demographics

HARSHIT SHARMA^{*}, SHAILY ROY^{*}, ASIF SALEKIN, Arizona State University, USA

Modern human-sensing applications often rely on data distributed across users and devices, where privacy concerns prevent centralized training. Federated Learning (FL) addresses this challenge by enabling collaborative model training without exposing raw data or attributes. However, achieving fairness in such settings remains difficult, as most human-sensing datasets lack demographic labels, and FL’s privacy guarantees limit the use of sensitive attributes. This paper introduces **CurvFed**: Curvature-Aligned Federated Learning for Fairness without Demographics, a theoretically grounded framework that promotes fairness in FL without requiring any demographic or sensitive attribute information—a concept termed *Fairness without Demographics (FWD)*—by optimizing the underlying loss-landscape curvature. Building on the theory that equivalent loss-landscape curvature corresponds to consistent model efficacy across sensitive attribute groups, **CurvFed** regularizes the top eigenvalue of the Fisher Information Matrix (FIM) as an efficient proxy for loss-landscape curvature, both within and across clients. This alignment promotes uniform model behavior across diverse bias-inducing factors, offering an attribute-agnostic route to algorithmic fairness. **CurvFed** is especially suitable for real-world human-sensing FL scenarios involving single or multi-user edge devices with unknown or multiple bias factors. We validated **CurvFed** through theoretical and empirical justifications, as well as comprehensive evaluations using three real-world datasets and a deployment on a heterogeneous testbed of resource-constrained devices. Additionally, we conduct sensitivity analyses on local training data volume, client sampling, communication overhead, resource costs, and runtime performance to demonstrate its feasibility for practical FL edge device deployment.

ACM Reference Format:

Harshit Sharma^{*}, Shaily Roy^{*}, Asif Salekin. 2018. CurvFed: Curvature-Aligned Federated Learning for Fairness without Demographics. In *Proceedings of Make sure to enter the correct conference title from your rights confirmation email (Conference acronym ’XX)*. ACM, New York, NY, USA, 44 pages. <https://doi.org/XXXXXXXX.XXXXXXX>

1 Introduction

The integration of advanced machine learning (ML) with ubiquitous sensing [47, 69] has enabled everyday devices like smartphones and wearables to collect rich data for human-centric applications, from gesture recognition [105] to stress detection [83]. Concurrently, edge and distributed computing—especially federated learning (FL)—have emerged as key frameworks for decentralized model training [60, 107]. In FL, each client (e.g., device or organization) retains local data and trains models privately [50], reducing centralization risks [5] and aligning with privacy regulations like GDPR, CCPA, and HIPAA [1, 100]. This makes FL ideal for human-sensing applications like health monitoring and activity recognition [22, 41, 76].

^{*}Equal Contribution.

Author’s Contact Information: Harshit Sharma^{*}, Shaily Roy^{*}, Asif Salekin, Arizona State University, Tempe, AZ, USA, {hsharm62,shailyro, asalekin}@asu.edu.

Permission to make digital or hard copies of all or part of this work for personal or classroom use is granted without fee provided that copies are not made or distributed for profit or commercial advantage and that copies bear this notice and the full citation on the first page. Copyrights for components of this work owned by others than the author(s) must be honored. Abstracting with credit is permitted. To copy otherwise, or republish, to post on servers or to redistribute to lists, requires prior specific permission and/or a fee. Request permissions from permissions@acm.org.

Conference acronym ’XX, Woodstock, NY

© 2018 Copyright held by the owner/author(s). Publication rights licensed to ACM.

ACM ISBN 978-1-4503-XXXX-X/2018/06

<https://doi.org/XXXXXXXX.XXXXXXX>

Notably, recent studies have begun exploring fairness in human-sensing federated learning (FL) [91, 95, 101]. However, state-of-the-art FL fairness approaches face a key challenge due to the trade-off between fairness and privacy [11], often requiring access to sensitive information at the client or server level, which contradicts *FL's privacy-preserving nature* [18, 23, 65, 99, 100]. This underscores the need for fairness-enhancing approaches that do not rely on sensitive or bias-inducing attributes. In human-sensing FL, this is especially important, as unlabeled factors can bias models—e.g., building materials can skew Wi-Fi CSI-based activity detection [45].

These challenges motivate the pursuit of Fairness without Demographics (FWD) [42]—refers to achieving equitable model performance across users or groups without relying on sensitive or demographic attributes such as sex, age, materials, among others, in FL, particularly since most human-sensing datasets lack labeled sensitive attributes [61, 95, 101]. *This also aligns with the 2025 Executive Order's [33] vision* for bias-resistant, innovation-driven AI by promoting fairness through optimization principles—without relying on demographic or group attributes—supporting equitable systems free from engineered social agendas. While FWD has been studied in centralized AI training [10, 30, 42], and only one FWD in FL work named FedSRCVaR [66] exists, FWD's integration into *privacy-preserving* decentralized FL remains challenging in human-centric FL, as outlined below:

- (1) Centralized FWD methods (Section 2.2) depend on access to global data distributions to identify biases and adjust decision boundaries, which is unavailable in *privacy-preserving* FL where clients only access local data [2], making fairness enforcement more difficult.
- (2) Although FedSRCVaR [66] does not require sensitive attribute labels in data, it relies on the knowledge of the bounds for sensitive or worst-case group sizes, making it not entirely agnostic to sensitive attribute knowledge (see Section 2.2).
- (3) Traditional group fairness methods—including FWD approaches (Section 2.2)—generally assume that all sensitive groups are represented during optimization [72]. However, this assumption is impractical in human-sensing FL, where each client often corresponds to a single user or a narrow demographic segment, resulting in an incomplete representation of population-level groups.
- (4) In human-centric sensing, multiple latent biases (e.g., gender, body type, sensor placement) coexist [36], and mitigating one bias may inadvertently worsen another [18].

In summary, a practical FWD solution for privacy-preserving human-sensing FL must operate without the knowledge of the sensitive attributes, tolerate missing group representations, and ensure fairness across both single- and multi- user clients and multiple bias sources. To address these challenges, this paper takes a fundamentally different approach than the literature—examining the *optimization loss-landscape geometry* of FL. It presents a theoretical justification (in Section 3) that reducing disparities in loss-landscape curvature both across and within clients offers an attribute-agnostic route to algorithmic fairness.

Building on this insight, it introduces *Curvature-Aligned Federated Learning (CurvFed)*, a novel FL method that achieves Fairness Without Demographics (FWD) by promoting *equitable and flatter* loss landscape curvatures across and within clients, without relying on sensitive attributes, bias factors, or global distribution knowledge, thus addressing the above-discussed first two and fourth challenges.

CurvFed utilizes the Fisher Information Matrix (FIM) as a fast-computable proxy for loss-landscape sharpness [44, 79], making it well-suited for resource-constrained edge devices (as FL clients), where it regularizes locally trained models to enhance fairness. Importantly, it introduces a sharpness-aware aggregation scheme, which aligns loss-landscape curvature across all clients by leveraging client-wise FIM data. This addresses the above-discussed third challenge, since FIM can be computed for both single-user and multi-user clients, allowing *CurvFed* to operate without requiring full representation of sensitive attributes within each client.

Recognizing the discussed challenges, our work introduces the first FWD for human-sensing FL, *CurvFed* that provides a privacy-preserving, robust alternative to traditional FL bias mitigation for human-sensing applications through the following contributions:

- *Theoretically Grounded Novel Approach: **CurvFed***, being the first of its kind, provides a comprehensive theoretical justification establishing how having flatter curvature within the client through local training and equitable curvatures across clients through a novel sharpness-aware aggregation scheme promotes FWD (Section 3). Its theoretical claims are further supported by empirical validation (Section 7), making it a rigorous and novel solution.
- *Superior fairness–accuracy tradeoff*: Existing FL methods often struggle with the inherent tension between fairness and accuracy [23, 27]. **CurvFed** mitigates this by promoting flatter loss landscapes during client training, which inherently enhances generalizability [16, 35] and model inference confidence by pushing samples away from decision boundaries [81]. It further optimizes both curvature smoothness and accuracy during aggregation, yielding a better balance of fairness and performance (see Sections 4.1 and 5.3, RQ-1).
- *Equitable performance across diverse FL setups*: **CurvFed** handles varying client compositions from single-user to multi-user, without requiring full representation of sensitive groups, ensuring practical and equitable performance in real-world human-sensing FL (see Section 5.3, RQ-2, RQ-3).
- *Improved multi-attribute fairness simultaneously*: Human-sensing data involves multiple sensitive attributes [23, 100], but fair FL methods struggle to address them simultaneously [15, 100]. **CurvFed** promotes flatter client loss landscapes, improving fairness across all attributes without relying on attribute labels (see Section 5.3, RQ-4).
- *Real-world feasibility and sensitivity analysis*: We validate **CurvFed**'s practicality through extensive evaluations across data volume, client sampling, communication cost, resource usage, and runtime on diverse platforms. Additionally, a *real-world testbed evaluation* on a heterogeneous testbed of six edge devices confirms its effectiveness under non-simulated conditions (see Sections 6 and 6.2).

We demonstrate the effectiveness of **CurvFed** across *three* real-world human-sensing datasets, each representing different sensing modalities, applications, and sensitive attributes, showing **CurvFed**'s effectiveness in FWD. We adopt off-the-shelf models previously published for these datasets [12, 90, 105] for FL setting. However, **CurvFed** is architecture-agnostic. The framework is not tied to specific model choices and can be readily extended to diverse use cases and architectures. *The rest of the paper is organized as follows*: Section 2 reviews prior work; Section 3 presents the theoretical foundation and assumptions of **CurvFed**; Section 3.1 defines the problem, gaps, and challenges. Section 4 details the proposed method, Section 5 presents in-depth results, Section 7 presents empirical verifications of our propositions, and Section 8 discusses broader impacts and limitations.

2 Background and Related works

Fairness has emerged as a critical concern in machine learning (ML) research, with early efforts focusing on pre-processing strategies, such as removing sensitive attributes from training data [21]. However, such approaches often compromise model performance [100], prompting a shift toward in-processing methods that embed fairness constraints into model optimization [104]. While effective in centralized ML, these methods face new challenges in federated learning (FL), where privacy constraints limit access to sensitive attributes [18, 67]. This section discusses the recent fairness approaches in FL, highlights common evaluation metrics, and motivates the need for Fairness Without Demographics (FWD).

2.1 Fairness in Federated Learning

Bias in FL systems can arise in multiple ways [15, 18, 52, 99, 106], but a primary concern is **performance-based group fairness**, which aims to reduce disparities in model performance across demographic groups [9]. This is distinct from **contribution fairness**, which addresses disparities from client participation or data imbalance (e.g., non-IID data) [52, 106], and is beyond the scope of this work. In this study, we align with performance-based

group fairness approaches and focus on *ensuring that the global model does not disproportionately underperform for any groups*, a challenge exacerbated by the decentralized nature of data in FL.

Group fairness approaches in FL can be categorized by where the intervention occurs: at the client, at the server, or both.

Client-Side and Hybrid Approaches: Several methods enforce fairness during local training. For example, FedFB applies fair batch sampling on the client side [99], while others use min-max optimization to minimize worst-case group loss [20, 62, 65]. However, these approaches typically require access to sensitive attribute labels, making them unsuitable for Fairness Without Demographics (FWD). Notably, AFL [62] targets fairness across clients, rather than demographic groups, whereas others assume the availability of knowledge of sensitive group labels and distributions.

Recent works that implicitly flatten the loss landscape offer a closer fit to our setting, as they can promote fairness without accessing sensitive data. For example, [8] applies Sharpness-Aware Minimization (SAM) at the client and Stochastic Weight Averaging (SWA) at the server. These methods, which do not rely on demographic attributes, serve as relevant baselines for our evaluations. Our approach, *CurvFed*, explicitly leverages sharpness cues and follows a hybrid framework leveraging sharpness information from the loss surface (a manner distinct from SAM) and adapting SWA in one of the modules. Our ablation study in Section 6.3 also demonstrates the impact of such adaptation in *CurvFed*.

Server-Side Approaches: Some strategies address fairness during the server’s aggregation phase. FairFed [23] adjusts model aggregation weights based on local fairness evaluations performed by clients. Similarly, Astral [18] uses an evolutionary algorithm to select clients for aggregation to promote fairness. While these methods maintain data decentralization, they still require clients to compute fairness metrics using sensitive group information, creating potential privacy risks and conflicting with the goals of FWD.

2.2 Fairness Without Demographics (FWD)

The challenge of achieving fairness without access to sensitive attributes has motivated the field of Fairness Without Demographics (FWD). In centralized ML, this has been explored through techniques like adversarial re-weighting to boost the importance of underperforming instances [42]. However, in FL, each client operates with its own training instances, making it challenging to identify such instances and apply this approach directly. Another approach, knowledge distillation (KD), was used by [10] to transfer knowledge from a complex teacher to a student model to improve fairness without accessing sensitive information. We adapt this KD concept to FL as a baseline. After initial few rounds of initial training via the FedAvg [60] protocol, each client subsequently performs KD using the global model as the teacher, training a local student model on its own data with soft labels from the teacher before sharing their local model for aggregation.

To our knowledge, the only existing work applying FWD directly to FL is FedSRCVaR [66]. While both our work and FedSRCVaR target fairness without sensitive attributes, their problem formulations differ fundamentally. FedSRCVaR adopts a Rawlsian approach [42], optimizing for a worst-performing subset of individuals defined by a tunable threshold, ρ . Selecting an appropriate ρ is non-trivial in heterogeneous FL settings and requires prior knowledge or extensive tuning [28]. Furthermore, its evaluation assumes each client represents a single sensitive group. In contrast, our setting assumes clients may have mixed or sparse group representations. Despite a lack of public implementation details, we adapted FedSRCVaR to our setting and report it as a key baseline for a comprehensive evaluation. Our method, *CurvFed*, differs by not imposing constraints on group size, offering a more flexible FWD approach.

2.3 A Loss landscape Primer

The *loss landscape* refers to the geometry of the objective function (or loss) mapped over the high-dimensional space of model parameters. The geometric properties of this landscape, particularly around the local minima found during training, are critical indicators of model performance [49].

Curvature and Sharpness: *Curvature* describes the rate at which the loss function changes as model parameters are perturbed[49]. Mathematically, this is characterized by the Hessian matrix (the matrix of second-order derivatives) of the loss function[73, 81]. Regions with high curvature are often referred to as *sharp* minima, where small changes in parameters lead to significant increases in loss. Conversely, *flat* minima are regions with low curvature, where the loss remains relatively stable despite parameter perturbations.

Connection to Model overfitting: Prior research has established a strong link between the geometry of the loss landscape and model generalization. "Flat" minima are generally associated with better generalization to unseen data, as they indicate a solution that is robust to shifts in the data distribution or noisy parameter updates [31, 39]. In contrast, sharp minima often lead to *model overfitting* [39, 87].

Measuring Curvature: While the Hessian provides a precise measure of curvature, computing it is computationally prohibitive for deep neural networks [78]. In this work, we utilize the top eigenvalue of the Fisher Information Matrix (FIM) as a computationally efficient proxy for the Hessian's top eigenvalue (and thus, the sharpness) [37, 53]. This metric allows us to quantify and align the "flatness" of models across federated clients without incurring the heavy cost of full Hessian computation.

2.4 Evaluation Metrics

We adopt established metrics to assess fairness and its trade-off with accuracy in FL [13, 17, 23, 48, 92].

Fairness: We use the **Equal Opportunity (EO) gap** [17, 23], defined as:

$$\Delta_{EO} = P(\hat{Y} = 1 \mid S = 1, Y = 1) - P(\hat{Y} = 1 \mid S = 0, Y = 1) \quad (1)$$

where \hat{Y} denotes the model's predicted label, Y the ground-truth label, and $S \in \{0, 1\}$ the binary sensitive attribute (e.g., sex or hand). The EO gap measures disparities in true positive rates across sensitive groups; a lower Δ_{EO} indicates greater fairness. Sensitive attributes are used only during post-training evaluation.

Fairness–Accuracy Trade-off: To evaluate balance, we use the **FATE** score [13, 48, 92], defined as:

$$\text{FATE} = \frac{\text{ACC}_m - \text{ACC}_b}{\text{ACC}_b} - \frac{\text{EO}_m - \text{EO}_b}{\text{EO}_b} \quad (2)$$

where ACC denotes classification accuracy, EO the Equal Opportunity gap, subscript m refers to the fair model, and subscript b denotes the baseline method (FedAvg [60]). The FATE score jointly captures relative accuracy gains and fairness improvements; higher values indicate a more favorable fairness–accuracy trade-off.

3 Theoretical Justification of *CurvFed*

This section theoretically justifies and highlights *CurvFed*'s novelty starting from the problem setting, literature gaps, and challenges. Finally, it outlines the study assumptions.

3.1 Problem Context and Literature Gap

Fair FL Setting: In a human-sensing fair FL framework, a central server coordinates training across q distributed edge platforms, referred to as clients. Each client $t \in \{1, 2, \dots, q\}$ holds its own local dataset \mathcal{D}_t , which may contain data from *one or more individuals*. Each client private dataset, $\mathcal{D}_t = \{(x_k, y_k)\}_{k=1}^{n_t}$, where x_k is an input instance, y_k is the corresponding label, n_t is the number of data instances for the client t .

We can consider \mathcal{D}_t as a union of m disjoint groups, $\mathcal{D}_t = \bigcup_{i=1}^m G_i$, where each group G_i represents a subset of data distinguished by attributes such as, demographic characteristics (e.g., sex, age) or contextual factors (e.g.,

sensor placement or orientation). The goal of *performance-based group fairness in this fair FL framework* is to ensure that all such groups—regardless of which client they belong to—receive similar model performance.

Each client t trains a local model using \mathcal{D}_t with parameters θ_t^* by minimizing an empirical risk function $J(\theta, \mathcal{D}_t)$, which represents the average empirical loss over the local dataset,

$$\begin{aligned} \theta_t^* &= \arg \min_{\theta} J(\theta, \mathcal{D}_t) \\ &= \arg \min_{\theta} \frac{1}{|\mathcal{D}_t|} \sum_i^{n_t} \ell(f_{\theta}(x_i), y_i) \end{aligned} \quad (3)$$

Here, f_{θ} is the predictive model parameterized by θ , and $\ell(\cdot)$ denotes a non-negative loss function that evaluates prediction error.

After local training, the server aggregates the client models $\{\theta_1^*, \dots, \theta_q^*\}$ into a global model with parameter θ^* . This aggregation is typically done through a weighted average, as shown in Eq. 4, where each client is assigned a non-negative weight β_t such that $\sum_{t=1}^q \beta_t = 1$, with the goal of minimizing its *excessive loss* (R) [66], shown in Eq. 5.

$$\theta^* = \sum_{t=1}^q \beta_t \theta_t^* \quad (4)$$

$$R(t) := J(\theta^*, \mathcal{D}_t) - J(\theta_t^*, \mathcal{D}_t) \quad (5)$$

Here, θ_t^* denotes the locally optimal model parameters obtained by client t , whereas θ^* represents the aggregated global model parameters produced by the central server. The excessive loss $R(t)$ quantifies the performance degradation experienced by client t when using the global model instead of its locally optimized model, evaluated on \mathcal{D}_t .

A key fairness concern is that the global model may disproportionately favor some clients. To address this, prior work [66] introduces the concept of excessive loss in Eq. 5—the performance gap between a client’s local and the global model—and promotes fairness by minimizing its variance across clients :

$$\arg \min \text{Var}_t [R(t)] = \frac{1}{q} \sum_{t=1}^q (R(t) - \bar{R})^2, \quad \text{where} \quad \bar{R} = \frac{1}{q} \sum_{t=1}^q R(t) \quad (6)$$

where, the operator $\text{Var}_t [\cdot]$ denotes variance computed across all clients indexed by $t \in \{1, \dots, q\}$.

This objective ensures that model utility is distributed equitably across clients. Throughout this work, $\|\cdot\|$ denotes the Euclidean norm, vectors and matrices are represented by bold symbols, and sets are denoted by uppercase letters, unless stated otherwise.

Challenge of this paper’s FWD problem setting: Our FWD objective is to promote fairness in FL beyond the scope discussed above. We aim to minimize disparities in model performance across all groups of individuals—regardless of which client they belong to—even when sensitive attributes (e.g., sex, age) that constitute the groups or underlie the disparities are unknown, latent, or unavailable. This consideration is especially critical in human-sensing applications, where a single client may represent data from one or more individuals with diverse and often unobservable characteristics. Consequently, achieving uniform performance across clients does not guarantee equitable treatment for all underlying groups or individuals. Our proposed solution builds on Eq. 6 to attain this FWD objective.

3.2 FWD in FL: A Curvature-Based Roadmap

We begin by establishing an upper bound on a client’s excessive loss Eq. 5, which helps isolate the disparity factors in terms of loss curvature within the client’s data, \mathcal{D}_t , and between the client’s and the global model. The following theorem and justifications assume that the loss function $\ell(\cdot)$ is at least twice differentiable, as is common for standard objectives such as cross-entropy and mean squared error.

Theorem 1 Through Taylor expansion, the upper bound of excessive loss $R(t)$ of the global model with parameters θ^* computed using client t ’s private dataset, \mathcal{D}_t is formalized as:

$$R(t) \leq \|g_t^\ell\| \times \|\theta^* - \theta_t^*\| + \frac{1}{2} \lambda(\mathbf{H}_t^\ell) \times \|\theta^* - \theta_t^*\|^2 + O(\|\theta^* - \theta_t^*\|^3). \quad (7)$$

Here, $g_t^\ell = \nabla_\theta \ell(\theta_t^*, \mathcal{D}_t)$ is the local models gradient vector, and $\mathbf{H}_t^\ell = \nabla_\theta^2 \ell(\theta_t^*, \mathcal{D}_t)$ is the local model’s Hessian at optimal parameter θ_t^* associated with the loss function ℓ . The term $\lambda(\cdot)$ denotes the maximum eigenvalue (hereby referenced as the top eigenvalue) and the big-oh term $O(\|\theta^* - \theta_t^*\|^3)$ represents all the higher order terms in the expansion. Equation 7 reveals that the excessive loss is tightly linked to the client t ’s (i) gradient vector corresponding to the loss, i.e., g_t^ℓ and (ii) the top Hessian eigenvalue, a proxy of the curvature (sharpness) of the local loss landscape.

Sharpness, Curvature, and Fairness: High curvature in the loss landscape of model optimization, characterized by sharp minima, typically associated with large top Hessian eigenvalues—is known to impair generalization [16, 35]. Importantly, disparities in two groups (based on demography or other factors) in terms of their top Hessian eigenvalues have been shown to correlate with the model’s performance disparities between those groups [81], suggesting that mitigating disparities among all groups’ curvatures (top Hessian eigenvalues) will promote fairness.

However, *there are several challenges to implementing this:*

- (1) Computing the full Hessian matrix is computationally costly [19], thus, infeasible on resource-constrained edge devices.
- (2) For us, the groups are unknown, because we are unaware of the factors (sensitive attributes) creating disparities.
- (3) In our setting, some clients can be just one person, implying all data can belong to just one group (at least in terms of demography or individual attributes like left or right-handed).

To address these challenges, we developed **CurvFed** — a principled framework that achieves fairness without explicit sensitive attribute labels (or knowledge) by regulating sharpness at both local client-level and global levels during model aggregation. Our method is guided by the following three propositions:

Proposition 1. Fisher Approximates Hessian

To address the *first challenge*, we leverage the empirical Fisher Information Matrix (FIM) as an efficient proxy for the Hessian:

$$\mathbf{H} \approx \mathbf{F} = \frac{1}{n_t} \sum_{i=1}^{n_t} \nabla_\theta \ell(f_\theta(x_i), y_i) \nabla_\theta \ell(f_\theta(x_i), y_i)^T. \quad (8)$$

For notational simplicity, \mathbf{H} here denotes the client-specific Hessian \mathbf{H}_t^ℓ evaluated at θ_t^* .

Lee et. al. [44] describe the relationship between the empirical FIM (\mathbf{F}) and the Hessian matrix (\mathbf{H}) as shown in equation 8. Where $\nabla_\theta \ell(f_\theta(x_i), y_i)$ is the the gradient vector corresponding to the loss of the i^{th} data sample, for a model f with parameters θ and the total number of data samples represented by n_t . The empirical FIM thus serves as a *computationally efficient* approximation of the Hessian, reducing computational costs during training [44, 78].

Proposition 2. Minimizing the FIM Top Eigenvalue Reduces Group-wise Curvature Disparity.

Building on Proposition 1, which establishes the FIM as a tractable approximation of the Hessian, we now provide a theoretical argument that minimizing the top eigenvalue of the FIM (denoted as $\lambda(F_t)$) during client-level training reduces curvature disparity across all constituent groups G_1, G_2, \dots, G_m within the local dataset $\mathcal{D}_t = \bigcup_{i=1}^m G_i$.

The full-dataset FIM can be expressed as a convex combination of group FIMs:

$$F_t = \sum_{i=1}^m \alpha_i F_{G_i}, \quad \text{where } \alpha_i = \frac{|G_i|}{|\mathcal{D}_t|}, \quad \sum_i \alpha_i = 1. \quad (9)$$

Using Jensen's and Weyl's inequalities [7, 32], with an assumption of approximate dominant eigenvector alignment for the lower bound, we establish bounds:

$$\max_i \lambda(F_{G_i}) - \delta \leq \lambda(F_t) \leq \sum_{i=1}^m \alpha_i \lambda(F_{G_i}) \quad (10)$$

where $\delta \geq 0$ accounts for potential eigenvector misalignment.

Our key insight is that during client training, penalizing $\lambda(F_t)$ implicitly drives the groups' top eigenvalues $\lambda(F_{G_i})$ towards uniformity. Notably, as shown in Eq. 10, minimizing $\lambda(F_t)$ effectively reduces the top eigenvalue of the group with the highest curvature, i.e., highest top eigenvalue of FIM ($\max_i \lambda(F_{G_i}) - \delta$). Intuitively, in the loss landscape, continuing to lower the dominant curvature reduces the variance across all groups' curvatures, promoting uniformity. *This approach is group-agnostic, relying purely on optimization geometry, thus addressing the second challenge discussed above.* Notably, empirical evidence supporting this theoretical reduction in curvature disparity is presented in Section 7.

Proposition 3. Sharpness-Aware Aggregation Reduces Variance in Excessive Loss Across Clients.

Building upon the understanding of excessive loss $R(t)$ from Theorem 1 and the local curvature control from Proposition 2, we now posit that our sharpness-aware aggregation scheme directly contributes to reducing the variance of excessive loss, $\text{Var}_t[R(t)]$, across clients—both in terms of performance and curvature. This promotes fairer performance distribution.

From Theorem 1 and Proposition 2, and assuming that the discrepancy $\delta_t = \|\theta^* - \theta_t^*\|$ remains sufficiently small—since the local training across clients occurs for a few epochs before each aggregation (allowing us to neglect higher-order terms and its variances), the excessive loss for client t is approximately:

$$R(t) \leq \|g_t^\ell\| \cdot \delta_t + \frac{1}{2} \lambda(F_t^\ell) \cdot \delta_t^2$$

Here, The quantity δ_t measures the parameter-space deviation between the global model and client t 's locally optimal model. g_t^ℓ is the local model's gradient at its optimum θ_t^* , and $\lambda(F_t^\ell)$ is the top eigenvalue of its FIM, serving as a proxy for Hessian's top eigenvalue (following Proposition 1). This indicates that for a client t , its excessive loss is impacted mostly by g_t^ℓ and $\lambda(F_t^\ell)$, which may vary significantly across clients. Our variance reduction strategy builds on this observation. During its local training, each client t seeks to minimize its empirical risk $J(\theta, \mathcal{D}_t)$. Successful training results in a small local gradient norm $\|g_t^\ell\|$ at θ_t^* . Furthermore, as established in Proposition 2, our framework encourages clients to find solutions θ_t^* that also exhibit low curvature, i.e., a minimized $\lambda(F_t^\ell)$. That means an effective locally trained client will have lower g_t^ℓ and $\lambda(F_t^\ell)$, thus lower excessive loss, and the opposite holds for ineffective locally trained ones.

CurvFed's Sharpness-Aware Aggregation builds on standard fair FL aggregation (Eq. 4-6) with the novel incorporation of curvature information into the weighting scheme. Specifically, client weights β_t in Eq. 4 are computed based on excessive loss $R(t)$, which accounts for both the local loss (corresponding to g_t) and top FIM eigenvalue $\lambda(F_t)$ (detailed in Section 4.1.2). Clients with lower $R(t)$, i.e., lower g_t and $\lambda(F_t)$ receive higher weights. This serves two goals: First, it *prioritizes effectively trained clients*—those with low loss (indicated by small g_t) and

low curvature $\lambda(F_t^{\ell})$, indicating locally fairer. These clients contribute more to the global model, resulting in lower and more uniform excessive loss $R(t)$ across them. And Second, the scheme effectively *mitigates "outlier" influence*: conversely, clients that exhibit high $R(t)$, which would lead to a higher $\text{Var}_t[R(t)]$, are assigned lower weights, curtailing their ability to inflate the $\text{Var}_t[R(t)]$ in Eq. 6.

Because the aggregation is driven by excessive loss, *CurvFed is agnostic to demographic (i.e., sensitive attributes) knowledge and the number of individuals belonging to clients, addressing challenges 2 and 3 discussed above*. In summary, by emphasizing well-trained, low-curvature clients, CurvFed reduces $\text{Var}_t[R(t)]$ in Eq. 6, guiding the global model toward fairer convergence, promoting group fairness without explicit demographic (i.e., sensitive attributes) knowledge.

3.3 Synthesis of Theoretical Insights: Curvature Alignment as a Proxy for Fairness Without Demographics (FWD) in Human-centric federated learning (FL)

The above theoretical results motivate curvature alignment as a principled and operational mechanism for achieving fairness under the challenging setting of FWD in human-centric FL.

As discussed in Section 2.1, conventional fairness-attaining approaches rely on explicit group-based metrics (e.g., the Equal Opportunity gap), which require access to sensitive or bias-inducing attribute labels. In our FWD setting, such labels are unavailable during training, and FL privacy constraints prohibit their use. Therefore, standard group-equalization strategies are not implementable. Moreover, human-sensing systems often involve multiple simultaneous bias-inducing factors (e.g., sex, body type, sensor placement) [36], and mitigating one explicitly may exacerbate another [18]. Therefore, this paper's challenge becomes more complex: ensuring fairness under unknown and potentially multi-attribute biases, rather than across predefined groups with known sensitive attributes.

Under these constraints, we pursue an alternative pathway grounded in recent ML optimization theories linking loss-landscape geometry to group-wise performance disparities. As Section 3, establishes that a client's local model's loss landscape curvature being flatter reduces disparities in generalization performance across groups within that client's local data (within client disparity reduction established through Theorem 1 and Proposition 1), and the loss landscape curvatures being similar across clients' local models reduce disparities in generalization performance across clients' local data (inter-client established in Proposition 2). Thus, loss landscape curvature is not treated as fairness itself, but as a measurable, optimization-level quantity that upper bounds performance disparity in the absence of information about demographic or bias-creating factors.

In summary, by promoting (1) Flatter curvature within clients, we reduce intra-client (even unknown) group-wise disparity, and (2) Similar curvature across clients, we reduce inter-client local data performance disparities. These together provide an attribute-agnostic pathway toward fairness across groups, whether a single or multiple sensitive or demographic factors are creating the disparity.

Importantly, curvature information (via the FIM top eigenvalue) does not reveal demographic information and can be computed locally, satisfying the constraints of privacy-preserving fairness without demographic (FWD) scope of FL. This makes curvature geometric consistency a feasible operational mechanism to attain FWD, whereas conventional fairness mechanisms are not implementable under the same constraints.

3.4 Assumptions

This study operates under the following assumptions:

- (1) We consider a centralized FL setup where a server coordinates training without access to clients' local datasets \mathcal{D}_t . No external public datasets are assumed to approximate the overall data distribution.
- (2) Our goal is to promote **performance-based group fairness** by ensuring the global model performs equitably across groups defined by sensitive attributes (e.g., sex, age, sensor location). For a sensitive

attribute a , let $G_c^a = \{(x_i, y_i) \mid x_i \text{ belongs to the category } c\}$ with $c \in \{1, \dots, C_a\}$ -categories of a . Fairness entails minimizing performance disparities across these groups, such as ensuring similar accuracy for $G_{\text{male}}^{\text{sex}}$ and $G_{\text{female}}^{\text{sex}}$.

- (3) We assume the central server is not resource-constrained and, consistent with standard FL approaches (e.g., FedAvg[60]), can perform model aggregation efficiently.
- (4) We assume that clients permit sharing loss-landscape curvature statistics (e.g., the top FIM eigenvalue) during FL aggregation. These statistics capture aggregate optimization geometry and do not involve sharing raw data, gradients, or sensitive attributes. To the best of our knowledge, there is no evidence that such curvature summaries can be used to reconstruct demographic or sensitive attribute information; thus, satisfying the FWD setting.

4 *CurvFed*: Design Choices and Approach

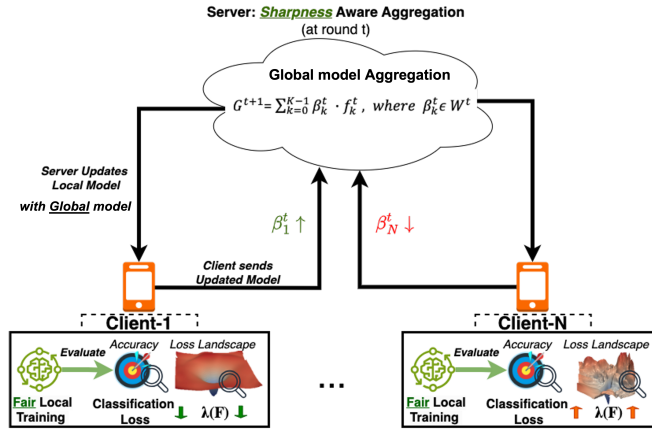


Fig. 1. Overview of *CurvFed*, illustrating client-side training, sharpness-aware aggregation, and global model updates in federated learning.

Fig. 1 provides an overview of *CurvFed*. In each FL round, clients use their own individuals' data to train local models, aiming to optimize accuracy and promote local fairness. The server then aggregates these models using our *Sharpness-aware aggregation* strategy to enhance fairness and accuracy. The global model is redistributed to clients for the next round. Details of *CurvFed* is below.

4.1 Design Choices

Our FWD attaining design choices leverage loss-landscape curvature at both client and global aggregation levels, grounded in the theoretical justifications in Section 3, are presented below:

4.1.1 Fair Local Training Objective: In the FL context, each client learns a model, denoted as f_{client} . We have two objectives on the client side: (1) maximizing accuracy and (2) promoting fairness, i.e., mitigating bias within the client's own data distribution.

We introduce a curvature regularization term in the client's loss function to enhance group fairness. The learning objective at the client-level is formulated as:

$$\begin{aligned} \arg \min \text{Loss}_{\text{client}} = & \alpha \cdot \ell_{\text{client}}(f_{\text{client}}(x_i)) \\ & + (1 - \alpha) \cdot \frac{1}{N_{\text{correct}}} \cdot \lambda(F^{\ell_{\text{client}}})_{\text{correct}} \end{aligned} \quad (11)$$

Here, N_{correct} represents the number of correctly classified instances in a batch, and x_i is the input in the i^{th} batch. The term $\ell_{\text{client}}(f_{\text{client}}(x_i))$ ensures accuracy maximization by minimizing classification loss. The regularization term penalizes the top eigenvalue of the FIM, i.e., $\lambda(F^{\ell_{\text{client}}})_{\text{correct}}$, associated with the loss for correctly classified samples, promoting group fairness as outlined in *Proposition 2* in Section 3.

In equation 11, we introduce α , a hyperparameter that acts as a balancing factor between the two objectives. α is identified using a grid search in this work. However, popular hyperparameter optimization frameworks like Optuna [3] can be used to find the optimal α . In our evaluations, the α values identified via grid search were effective across all three datasets, with one dataset exhibiting an optimal value within a similar range. A detailed discussion of the sensitivity to the weighting factor is provided in Section 6.2.4. This consistency suggests that the local optimization strategy transfers reasonably well across heterogeneous human-sensing datasets. We will use $\lambda(F_{\text{client}})$ instead of $\lambda(F^{\ell_{\text{client}}})_{\text{correct}}$ for simplicity for the rest of the section.

4.1.2 Sharpness-aware Aggregation to Promote Fairness: After local training, each client has a distinct accuracy and top eigenvalue of FIM ($\lambda(F_{\text{client}})$), as depicted in Fig. 1, leading to varying excessive losses. As outlined in *Proposition 3* in Section 3, clients with lower excessive losses should contribute more to deriving the aggregated global model.

This aggregation strategy draws inspiration from Pessimistic Weighted Aggregation (P-W) in FL [17], which excludes clients with known biases during aggregation. However, in the FWD setting, such bias information is unavailable. Instead, our *Sharpness-aware Aggregation* implicitly promotes fairness by assigning higher weights to clients with lower excessive loss, i.e., having lower top eigenvalue of FIM and lower classification error (according to *Proposition 3*), thus supporting fairer and more performant global updates without relying on explicit sensitive attributes.

To compute the aggregation weights for N clients: $W^r = \{\beta_n^r \mid \forall n \in \{1, \dots, N\}\}$ at each round r , the server collects each client's evaluation loss $\text{loss}_n^{\text{eval}}$ and the top FIM eigenvalue $\lambda(F_n^{\text{eval}})$. These are then used to compute the aggregation weights as described in Equation 12.

$$W^r = S(S(L) \cdot S(T)) \quad (12)$$

Here, we use the *Softmax operator* denoted as S for simplicity. Notably, $L = \left\{ \epsilon + \frac{1}{\text{loss}_n^{\text{eval}}} \right\}_{n=1}^N$ and $T = \left\{ \epsilon + \frac{1}{\lambda(F_n^{\text{eval}})} \right\}_{n=1}^N$ and ϵ is a small constant to avoid division by zero in weight calculations.

4.2 Approach

Algorithm 1 outlines **CurvFed** approach, which begins with the following inputs: a randomly initialized global model denoted as G^0 , the number of clients participating in FL process represented by N , the total number of rounds for the FL process indicated by R , the number of epochs E for conducting local training on each client's side, the cycle length c for implementing the stochastic weight averaging (SWA) protocol [8], the weighting factor α used to balance the client loss, the batch size B utilized by the clients during training, client learning rate γ and learning rate scheduler $\gamma(\cdot)$. Different modules of **CurvFed** are detailed below:

4.2.1 Local Client Training: Following standard FL protocol [60], the server initializes by distributing a randomly initialized global model G^0 and other training parameters to the clients for local training through the *TrainClient* module (line 12-13).

Algorithm 1 Curvature-Aligned Federated Learning (*CurvFed*)

```

1: Input:  $\diamond G^0$ : Initial random model,  $\diamond N$ : Number of Clients,  $\diamond R$ : Total rounds,  $\diamond E$ : local training epochs,  $\diamond c$ : cycle
   length,  $\diamond \eta$ : SWA starting threshold,  $\diamond \alpha$ : client loss weighting factor,  $\diamond B$ : Client batch size,  $\diamond \gamma$ : Learning rate,  $\diamond \gamma()$ :
   Learning rate scheduler
2: Parameter:  $\diamond L[]$ : Array to store classification loss of clients,  $\diamond T[]$ : Array to store top eigenvalue of FIM of clients,  $\diamond S$ :
   Softmax operator
3: Returns:  $G_{\text{SWA}}$ : Global model
4: for each round  $r=0$  to  $R-1$  do
5:   if  $r = \eta \times R$  then
6:      $G_{\text{SWA}} \leftarrow G^r$ 
7:   end if
8:   if  $n \geq \eta \times R$  then
9:      $\gamma = \gamma(r)$ 
10:  end if
11:  for each  $Client_n$   $n=0$  to  $N-1$  do
12:     $params \leftarrow G^r, Client_n, E, B, \alpha, \gamma$ 
13:     $f_n^r, loss_n^r, \lambda(F_n^r) \leftarrow TrainClient(params)$ 
14:     $L[n] \leftarrow \epsilon + \frac{1}{loss_n^r}$ 
15:     $T[k] \leftarrow \epsilon + \frac{1}{\lambda(F_n^r)}$ 
16:  end for
17:   $W^r = S(S(L) \cdot S(T))$ 
18:   $G^{r+1} = \sum_{n=1}^N \beta_n^r \cdot f_n^r \quad \forall \beta_n^r \in W^r$ 
19:  if  $r \geq \eta \times R$  and  $mod(r, c) = 0$  then
20:     $n_{models} \leftarrow n/c$ 
21:     $G_{\text{SWA}} \leftarrow \frac{n_{model} \times G_{\text{SWA}} + G^r}{n_{models} + 1}$ 
22:  end if
23: end for
24: return  $G_{\text{SWA}}$ 

```

TrainClient Module, as shown in Algorithm 2, receives the global model, along with training configurations such as the number of local training epochs E , batch size B , learning rate γ , and the client loss weighting factor α from the server. On the client side, data is divided into a training set \mathcal{D}_{train} and an evaluation set \mathcal{D}_{eval} . The model is trained on \mathcal{D}_{train} (line-9), where we utilized the Sharpness-Aware Minimization (SAM) optimizer for model training[25]. The choice of the model optimizer is influenced by prior works in FL, which claim that using SAM optimizer at the client level helps with convergence and promotes local flatness [8], thus lowering curvature and further promoting fairness.

The client-local training follows the dual objective discussed in Section 4.1.1, as per Equation 11. The model performance is assessed on the disjoint \mathcal{D}_{eval} (line-11) to identify the best-performing model. For this model, the evaluation loss $eval_loss_n$ and the top eigenvalue of the FIM $eval_ \lambda(F_n)$ are calculated. The optimal model's evaluation loss and FIM top eigenvalue are stored in $Loss_{eval,n}^r$ and $\lambda(F_{eval,n}^r)$, respectively (Lines 12,13). These metrics and the weights of the selected model are then sent back to the server (line-15).

4.2.2 Sharpness-aware Aggregation: Upon receipt of the clients' local training returns, as per Algorithm 1, the server starts the model aggregation phase. Our *Sharpness-aware aggregation* method calculates weights for each client based on their classification loss and the top eigenvalue of the FIM related to their loss (lines 14,15). Clients with lower classification loss and lower top eigenvalue of FIM are assigned higher weights (line 17).

Algorithm 2 $TrainClient(G^t, Client_k, E, B, \alpha, \gamma)$

```

1: Parameter:  $\diamond G^t$ : Initial model sent from Server side,  $\diamond E$ : local training epochs at Client side,  $\diamond Client_k$ : Client-ID,  $\diamond B$ :
   Client Batch size,  $\diamond \alpha$ : client loss weighting factor,  $\diamond \gamma$ : client learning rate
2: Returns:  $f_n^r, Loss_{eval,n}^r, \lambda(F_{eval,n}^r)$ 
3: Initialize:  $f_n^r \leftarrow G^r$  {Server-side global model}
4: Initialize:  $l_n$  {Client Classification loss}
5: Initialize: SAM optimizer
6: Split:  $Client_n$  data  $\mathcal{D}_n$  into  $\mathcal{D}_{train}$  and  $\mathcal{D}_{eval}$ 
7: for each epoch  $e=0$  to  $E-1$  do
8:   for each batch  $i=0$  to  $B$  in  $\mathcal{D}_{train}$  do
9:      $argminLoss_n$ 
10:   end for
11:   Evaluate  $f_n$  on  $\mathcal{D}_{eval}$  get:  $eval\_loss_n, eval\_l(F_n)$ 
12:    $Loss_{eval,n}^r \leftarrow eval\_loss_n$ 
13:    $\lambda(F_{eval,n}^r) \leftarrow eval\_l(F_n)$ 
14: end for
15: return  $f_n^r, Loss_{eval,n}^r, \lambda(F_{eval,n}^r)$ 

```

Stochastic Weight Averaging (SWA): On the server side, we also use SWA [34], a technique shown to enhance generalization in FL systems [8]. The significance of generalization in fair models is underscored by research [14, 24] focusing on improving their robustness and ability to perform fairly across unseen data. This addresses the challenge of fairness constraint overfitting [14], where models fair on training data may still exhibit unfairness on unseen data. In human-sensing FL, ensuring fairness and robustness across unseen instances is critical; hence, the adoption of SWA is crucial in *CurvFed*. SWA averages the global models at regular intervals, i.e., cycles c (line 19), and adjusts the learning rate throughout the FL process (line 9) to achieve flatter minima, thereby preventing overfitting as the process advances. The SWA process begins after a threshold (η) number of rounds are complete (lines 4-7); for our evaluations, this threshold is set to $\eta = 20\%$. The early start threshold was chosen due to the limited data size, which allows for quicker convergence in our setting.

5 Experimental Evaluation

This section provides a comprehensive evaluation of *CurvFed*, covering datasets and models (Section 5.1), followed by an analysis addressing four key research questions on CurvFed’s effectiveness (Section 5.3). In this work, we compared *CurvFed* against standard benign FL models—FedAvg[60], FedSAM [70], and FedSWA [8]—and two recent fairness-without-disparity (FWD) approaches: KD-FedAvg [10] (adopted for FL settings) and FedSRCVaR [66].

5.1 Evaluation Datasets

Dataset	Sensing Modality	# of Participants (N)	Application Task	Sensitive Attributes
WIDAR [105]	WiFi (CSI Velocity Profiles)	$N = 12$	Gesture Recognition	Sex, Sensor Orientation
HugaDB [12]	Inertial (Accel + Gyro)	$N = 18$	Human Activity Recognition	Sex
Stress Sensing [90]	Physiological (EDA + Accel)	$N = 48$	Stress Detection	Sex, Watch Hand
PERCEPT-R [6]	Audio (Speech)	$N = 76$	Clinical Speech Assessment	Sex

Table 1. Summary of datasets used for evaluation. The diversity in sensing modalities and tasks demonstrates the generalizability of *CurvFed* across the human-sensing spectrum.

We evaluate *CurvFed* on *four* heterogeneous human-sensing datasets, summarized in Table 1. These datasets were selected to test generalizability across diverse sensing modalities (WiFi, inertial, physiological, and audio) and distinct sensing tasks (HAR, stress detection, and speech therapy). Crucially, each dataset contains different sensitive attributes as biological sex, sensor placement, that challenge the fairness of standard FL algorithms [18, 95]. In all our evaluation, the sensitive attributes were used solely for *post-hoc fairness assessment*.

WIDAR (WiFi-based HAR): This dataset leverages Channel State Information (CSI) derived from WiFi signals [71] to capture body-coordinate velocity profiles during human activities [105]. Data were collected from 16 participants performing a set of gestures under varying conditions. To evaluate the robustness of *CurvFed*, we consider biological *sex* and receiver *orientation* as sources of natural variability across participants.

HugaDB (Inertial HAR): HugaDB [12] focuses on wearable activity recognition and comprises accelerometer and gyroscope data collected from body-worn sensors on 18 participants. The dataset provides a testbed for assessing whether *CurvFed* can achieve equitable performance across individuals with differing physiological characteristics, without relying on demographic information during training. For fairness evaluation purposes, biological *sex* is designated as the sensitive attribute.

Stress Sensing (Physiological): To evaluate multi-modal robustness, we utilize the Stress Sensing dataset [90] (48 participants). It combines electrodermal activity (EDA) and accelerometer readings from an Empatica E4 wristband [59] to detect stress events. Sensitive attributes include biological *sex* and the *hand* (left vs. right) on which the device was worn.

PERCEPT-R (Clinical Audio): We extend our evaluation to the digital health domain using a publicly available subset of the PERCEPT corpus (v2.2.2) [6]. The dataset consists of single-word speech recordings from children with speech sound disorders involving the rhotic /r/ sound. In collaboration with clinical experts, we curated a cohort of 76 participants and used expert-provided rhoticity annotations (0 = derhotic, 1 = fully rhotic). *Sex* is treated as the sensitive attribute to assess the equity of the clinical classification model across demographic groups. Further details on the datasets and FL client distributions for FL evaluations can be found in Appendix A.1.

5.2 Model Architectures and Hyper-parameters

We employ task-specific benchmark model architectures tailored to the computational constraints of edge devices and the specific modalities of each dataset.

HAR and Stress Sensing (MLPs): For the WIDAR, HugaDB, and Stress Sensing datasets, we adapt established benchmark architectures [68, 77, 93]. These are implemented as Multi-Layer Perceptrons (MLPs) with varying depth (2–3 layers) and regularization techniques (Dropout, Batch/Instance Normalization) optimized for their respective feature sets.

Clinical Audio (CNN): For the PERCEPT-R dataset, we utilized a Convolutional Neural Network (CNN) model [6] to process the temporal speech sequences. The network comprises two 1D convolutional layers (kernel size 5) that extract temporal features from the 5-channel input. The output is flattened and passed through a three-layer MLP classifier employing Hardswish activations to predict rhoticity.

Hyperparameters: We maintain consistent training budgets i.e. total number of FL rounds (R) and Local client training epochs (E) across all methods to ensure fair comparison. Table 2 details the specific hyperparameter settings for all four datasets. For the standard FedAvg, KD-Fedavg and FedSAM baselines, we utilize the "Base Learning Rate" and constant averaging. For *CurvFed* and FedSWA, we introduce the SWA components (SWA LR, α , Cycle). Notably, the PERCEPT-R dataset requires a distinct configuration (lower α , longer training) due to the higher complexity of the audio modality. Further details on grid search are provided in Appendix A.1.4.

Hyperparameter	WIDAR	Stress Sensing	HugaDB	PERCEPT-R
<i>Training Budget</i>				
Local Epochs (E)	3	3	3	5
Total Rounds (R)	80	80	80	100
<i>Optimization (CurvFed / Baseline)</i>				
Base Learning Rate (η)	0.01 / 0.1	0.01 / 0.1	0.001 / 0.001	0.001 / 0.001
SWA Learning Rate (η_{swa})	0.1	0.001	0.001	0.001
<i>Curvature Constraints (CurvFed)</i>				
Curvature Penalty (α)	0.92	0.92	0.92	0.8
Cycle Length (c)	5	5	3	5
SWA Start Round	16	16	16	20
Stability Constant (ϵ) (Eq 12)	0.005	0.005	0.005	0.005

Table 2. Hyperparameter configuration for main experiments. **CurvFed** introduces specific parameters (SWA, α) to manage curvature. All methods share the same epoch and round budget to ensure fair comparison.

5.3 Evaluation on **CurvFed**'s Effectiveness

To establish the effectiveness and stability of **CurvFed**, we conducted a comprehensive evaluation using **stratified 5-fold cross-validation** (maintaining an 80:20 train-test split per client), repeated across *three* distinct random seeds. To maintain clarity, we present the mean and standard deviation for both the F1 score and the EO gap, averaged across folds for a representative seed. Furthermore, we report the FATE score, which is calculated using the mean F1 and mean EO values as defined in Equation 2. Complete results for the additional seeds are provided in Appendix A.1.4. Our analysis is structured around the following research questions (RQs), each targeting a different aspect of fairness and efficacy in FL:

- **RQ-1:** Could **CurvFed** improve the fairness–efficacy balance compared to contemporary benign (i.e., non-fairness-aware) FL approaches or FWD FL baselines?
- **RQ-2:** Can fairness be achieved in FL settings that include both *single-person* and *multi-person* clients?
- **RQ-3:** Can **CurvFed** enhance fairness specifically for *single-person* clients?
- **RQ-4:** Could **CurvFed** improve fairness across *multiple sensitive attributes simultaneously*?

The following sections present a detailed analysis of each question.

5.3.1 RQ-1: Could **CurvFed improve the fairness–efficacy balance compared to contemporary benign FL approaches or FWD FL baselines?** We evaluated whether **CurvFed** improves the trade-off between predictive performance and fairness relative to existing federated learning baselines. Fairness is measured using the FATE score and the Equal Opportunity (EO) gap with respect to *sex*.

FedAvg is the fairness-unaware baseline, while FedSAM and FedSWA are benign baselines that promote flatter loss landscapes via client-side SAM and server-side SWA [8].

FL Client composition reflecting real-world disparities: WIDAR and HugaDB clients typically include four males and one female (with one HugaDB client having two males and one female), while Stress Sensing shows greater variation (e.g., 2:4 to 3:6 male:female ratios). Unless otherwise noted, this distribution is used throughout.

Evaluation discussion: As shown in Table 3, results are reported as the mean \pm standard deviation over 5-fold cross-validation. **CurvFed** consistently improves the fairness–efficacy trade-off across all datasets. In WIDAR, it reduces the EO gap from 0.412 ± 0.0154 (FedAvg) to 0.354 ± 0.0099 , with a moderate F1 reduction (0.806 ± 0.0458 vs. 0.862 ± 0.0006). In Stress Sensing, it improves both F1 (0.789 ± 0.0086 vs. 0.767 ± 0.0146) and EO gap (0.259 ± 0.0045 vs. 0.324 ± 0.014). HugaDB shows similar trends, with a higher F1 (0.892 ± 0.0072) and reduced EO gap (0.406 ± 0.0042) compared to FedAvg (0.852 ± 0.0063 , 0.482 ± 0.0294). In Percept-R, where baseline models exhibit comparable F1 performance, **CurvFed** achieves the lowest EO gap (0.106 ± 0.01) with only a small reduction in F1 (0.764 ± 0.003 vs. 0.777 ± 0.002 for FedAvg).

Dataset	Model	F1 Score	EO Gap	FATE $\times 10^{-1}$
		Mean \pm Std (\uparrow)	Mean \pm Std (\downarrow)	Mean Score (\uparrow)
WIDAR	FedAvg	0.862 \pm 0.0006	0.412 \pm 0.0154	0.0000
	FedSAM	0.843 \pm 0.0108	0.401 \pm 0.0230	0.056
	FedSWA	0.859 \pm 0.0030	0.405 \pm 0.0142	0.147
	FedSRCVaR	0.724 \pm 0.0187	0.345 \pm 0.0534	0.019
	KD-Fedavg	0.849 \pm 0.0123	0.392 \pm 0.0299	0.327
	CurvFed	0.806 \pm 0.0458	0.354 \pm 0.0099	0.741
Stress sensing	FedAvg	0.767 \pm 0.0146	0.3240 \pm 0.014	0.000
	FedSAM	0.784 \pm 0.0094	0.3135 \pm 0.0103	0.548
	FedSWA	0.743 \pm 0.0164	0.305 \pm 0.0034	0.257
	FedSRCVaR	0.694 \pm 0.0253	0.278 \pm 0.0231	0.458
	KD-Fedavg	0.717 \pm 0.0157	0.259 \pm 0.0095	1.344
	CurvFed	0.789 \pm 0.0086	0.259 \pm 0.0045	2.292
HugaDB	FedAvg	0.852 \pm 0.0063	0.482 \pm 0.0294	0.0000
	FedSAM	0.786 \pm 0.0034	0.438 \pm 0.0042	0.014
	FedSWA	0.809 \pm 0.0033	0.439 \pm 0.0144	0.040
	FedSRCVaR	0.862 \pm 0.0032	0.410 \pm 0.0103	0.163
	KD-Fedavg	0.776 \pm 0.0061	0.444 \pm 0.0161	-0.008
	CurvFed	0.892 \pm 0.0072	0.406 \pm 0.0042	0.206
Percept-R	FedAvg	0.7774 \pm 0.002	0.162 \pm 0.005	0.0000
	FedSAM	0.777 \pm 0.002	0.136 \pm 0.01	1.72
	FedSWA	0.777 \pm 0.002	0.127 \pm 0.01	1.66
	FedSRCVaR	0.771 \pm 0.004	0.130 \pm 0.01	1.73
	KD-Fedavg	0.777 \pm 0.001	0.150 \pm 0.01	0.76
	CurvFed	0.764 \pm 0.003	0.106 \pm 0.01	3.29

Table 3. Fairness–efficacy balance comparisons for RQ-1. Results are averaged over 5-fold cross-validation. Metrics with \uparrow indicate higher is better, while metrics with \downarrow indicate lower is better. CurvFed attains the highest FATE score, reflecting the overall fairness–utility balance

CurvFed consistently outperforms KD-FedAvg and FedSRCVaR in FATE scores across all datasets—Stress Sensing (2.292 vs. 1.344 and 0.458), WIDAR (0.741 vs. 0.327 and 0.019), HugaDB (0.206 vs. -0.008 and 0.163), and Percept-R (3.29 vs. 0.76 and 1.73). While KD-based methods excel in centralized settings with diverse group-wise data [10], their local fairness improvements do not reliably carry over after model aggregation in FL [29]. This limits their effectiveness in FL settings.

FedSRCVaR, relies on a constraint ρ to bound worst-case group sizes [66], assumes known group distributions—often unavailable in human-centric data with missing or highly variable groups across clients. This results in unstable optimization and poor fairness–utility trade-offs, as reflected by the reduced F1 score (0.694 \pm 0.0253) on the Stress Sensing dataset. In contrast, **CurvFed** makes no such assumptions and achieves better fairness–performance balance.

5.3.2 RQ-2: Can fairness be achieved in FL settings that include both single-person and multi-person clients?

Traditional fairness-aware FL methods assume each client contains data from all sensitive groups. However, as noted in Section 1 challenge 3, edge devices may contain data from a single user or multiple users. Thus, this assumption often fails in real-world deployments. Notably, **CurvFed** removes this assumption by promoting fairness through loss landscape regularization, making it impactful for practical deployment in human-sensing applications. Table 4 presents **CurvFed**'s performance across all four datasets, under a mix of single- and multi-person clients with 1–2 males and 0–1 females per client (See Appendix A.1.3 for detailed client distributions). Despite the absence of full group representation, **CurvFed** consistently outperforms other FL methods, achieving

strong FATE scores of 0.479×10^{-1} on WIDAR, 4.032×10^{-1} on Stress Sensing, 0.590×10^{-1} on HugaDB, and 2.03×10^{-1} on Percept-R, demonstrating balanced fairness and performance under practical constraints.

*5.3.3 RQ-3: Can **CurvFed** enhance fairness specifically for single-person clients?* Only single-person clients are common in human-centric FL but pose challenges due to the lack of intra-client diversity, making global fairness and performance difficult to achieve. Prior studies [56, 94] show that simple aggregation methods like FedAvg often degrade global performance in these cases [56].

Dataset	Client Type	Model	F1 Score	EO Gap	FATE $\times 10^{-1}$
			Mean \pm Std (\uparrow)	Mean \pm Std (\downarrow)	Mean (\uparrow)
WIDAR	Single & Multi-Person	FedAvg	0.836 \pm 0.0132	0.429 \pm 0.0081	0.000
		FedSAM	0.822 \pm 0.0143	0.411 \pm 0.0032	0.238
		FedSWA	0.852 \pm 0.0323	0.431 \pm 0.0034	0.140
		KD-FedAvg	0.781 \pm 0.0030	0.389 \pm 0.0013	0.270
		FedSRCVaR	0.712 \pm 0.0048	0.405 \pm 0.0112	-0.929
		CurvFed	0.791 \pm 0.0089	0.385 \pm 0.0089	0.479
	Single Person Only	FedAvg	0.843 \pm 0.0115	0.441 \pm 0.0143	0.000
		FedSAM	0.839 \pm 0.0053	0.423 \pm 0.0098	0.366
		FedSWA	0.842 \pm 0.0093	0.424 \pm 0.0034	0.383
		FedSRCVaR	0.706 \pm 0.0124	0.418 \pm 0.0075	-1.094
		KD-FedAvg	0.771 \pm 0.0119	0.402 \pm 0.0082	0.030
		CurvFed	0.793 \pm 0.0092	0.382 \pm 0.0045	0.754
Stress Sensing	Single & Multi-Person	FedAvg	0.761 \pm 0.0143	0.376 \pm 0.0023	0.000
		FedSAM	0.749 \pm 0.0034	0.382 \pm 0.0120	-0.313
		FedSWA	0.841 \pm 0.0145	0.310 \pm 0.0114	2.822
		KD-FedAvg	0.745 \pm 0.0129	0.248 \pm 0.0024	3.193
		FedSRCVaR	0.701 \pm 0.0083	0.283 \pm 0.0215	1.683
		CurvFed	0.829 \pm 0.0129	0.258 \pm 0.0134	4.032
	Single Person Only	FedAvg	0.762 \pm 0.0014	0.382 \pm 0.0034	0.000
		FedSAM	0.769 \pm 0.0093	0.338 \pm 0.0093	1.235
		FedSWA	0.779 \pm 0.0182	0.368 \pm 0.0076	0.589
		FedSRCVaR	0.675 \pm 0.0214	0.218 \pm 0.0142	3.143
		KD-FedAvg	0.680 \pm 0.0313	0.257 \pm 0.0117	2.186
		CurvFed	0.731 \pm 0.0362	0.235 \pm 0.0189	3.447
HugaDB	Single & Multi-Person	FedAvg	0.856 \pm 0.0113	0.441 \pm 0.0042	0.000
		FedSAM	0.847 \pm 0.0118	0.408 \pm 0.0032	0.636
		FedSWA	0.842 \pm 0.0092	0.413 \pm 0.0092	0.461
		KD-FedAvg	0.789 \pm 0.0068	0.409 \pm 0.0045	-0.048
		FedSRCVaR	0.827 \pm 0.0182	0.403 \pm 0.0142	0.524
		CurvFed	0.816 \pm 0.0340	0.395 \pm 0.0083	0.590
	Single Person Only	FedAvg	0.871 \pm 0.0013	0.454 \pm 0.0034	0.000
		FedSAM	0.856 \pm 0.0052	0.502 \pm 0.0182	-1.230
		FedSWA	0.783 \pm 0.0432	0.432 \pm 0.0231	-0.525
		FedSRCVaR	0.792 \pm 0.0092	0.411 \pm 0.0092	0.038
		KD-FedAvg	0.769 \pm 0.0082	0.409 \pm 0.0048	-0.180
		CurvFed	0.824 \pm 0.0054	0.418 \pm 0.0092	0.253
Percept-R	Single & Multi-Person	FedAvg	0.785 \pm 0.006	0.132 \pm 0.01	0.0000
		FedSAM	0.781 \pm 0.004	0.113 \pm 0.01	1.31
		FedSWA	0.780 \pm 0.004	0.117 \pm 0.01	1.02
		KD-FedAvg	0.784 \pm 0.006	0.132 \pm 0.01	-0.06
		FedSRCVaR	0.783 \pm 0.006	0.131 \pm 0.009	0.03
		CurvFed	0.772 \pm 0.003	0.102 \pm 0.01	2.03
	Single Person Only	FedAvg	0.770 \pm 0.005	0.108 \pm 0.01	0.0000
		FedSAM	0.768 \pm 0.006	0.115 \pm 0.008	-0.71
		FedSWA	0.765 \pm 0.007	0.112 \pm 0.008	-0.45
		FedSRCVaR	0.770 \pm 0.005	0.102 \pm 0.01	0.5
		KD-FedAvg	0.770 \pm 0.005	0.106 \pm 0.01	0.17
		CurvFed	0.764 \pm 0.007	0.054 \pm 0.004	4.85

Table 4. Performance comparison across different client setups: single & multi-person clients (RQ2) and single-person clients (RQ3). Results are averaged over 5-fold cross-validation. Metrics with \uparrow indicate higher is better, while metrics with \downarrow indicate lower is better. *Note: While some methods perform better on individual F1 or EO Gap metrics, CurvFed attains the highest FATE score, reflecting the overall fairness-utility balance*

We evaluated *CurvFed* against other FWD baselines in only single-client scenarios. As shown in Table 4, *CurvFed* consistently achieves the highest FATE scores across all datasets in this setting, including 0.754×10^{-1} for WIDAR, 3.447×10^{-1} for Stress Sensing, 0.253×10^{-1} for HugaDB, and 4.85×10^{-1} for Percept-R—demonstrating its effectiveness even without client-level sensitive attribute diversity.

5.3.4 RQ-4: Could *CurvFed* improve fairness across multiple sensitive attributes simultaneously? In FL-based human sensing, data often simultaneously involve multiple sensitive attributes (e.g., sex, age, body type, sensor placement). To assess *CurvFed* under such conditions, we evaluated fairness with respect to additional sensitive attributes—hands’ (watch-hand) and orientation’ (sensor placement)—in the Stress Sensing and WIDAR datasets, using the same models as in Table 3. For WIDAR, we induced disparity by subsampling 50% of data from orientations 4 and 5, grouping orientations 1–3 as "major" and the rest as "minor." In Stress Sensing, only 13 of 48 participants had both-hand data, while others had left-hand only. HugaDB and Percept_R, with only sex as a sensitive attribute, were excluded.

As shown in Table 5, *CurvFed* consistently achieves the strongest fairness–utility trade-off across both sensitive attributes. Although other methods may attain higher F1 scores or lower EO gaps individually, *CurvFed* maintains competitive classification performance while simultaneously reducing EO gaps, resulting in the highest FATE scores on both WIDAR and Stress Sensing. This indicates that *CurvFed* does not optimize a single objective in isolation but instead preserves a balanced trade-off between fairness and accuracy when multiple sensitive attributes are present, thereby addressing Challenge 4 outlined in Section 1.

Dataset	Sensitive Attribute	Model	F1 Score Mean \pm Std (\uparrow)	EO Gap Mean \pm Std (\downarrow)	FATE $\times 10^{-1}$ Mean (\uparrow)
WIDAR	Orientation	FedAvg	0.862 \pm 0.0006	0.506 \pm 0.0161	0.000
		FedSAM	0.843 \pm 0.0108	0.481 \pm 0.0146	0.284
		FedSWA	0.859 \pm 0.0030	0.499 \pm 0.0499	0.102
		FedSRCVaR	0.725 \pm 0.0187	0.422 \pm 0.0535	0.060
		KD-Fedavg	0.849 \pm 0.0123	0.458 \pm 0.0343	0.793
		CurvFed	0.806 \pm 0.0458	0.395 \pm 0.0507	1.550
Stress Sensing	Hand	FedAvg	0.767 \pm 0.0146	0.464 \pm 0.0124	0.000
		FedSAM	0.785 \pm 0.0094	0.463 \pm 0.0830	0.233
		FedSWA	0.744 \pm 0.0164	0.441 \pm 0.0234	0.173
		FedSRCVaR	0.695 \pm 0.0253	0.394 \pm 0.0211	0.550
		KD-Fedavg	0.718 \pm 0.0157	0.406 \pm 0.0193	0.587
		CurvFed	0.789 \pm 0.0086	0.433 \pm 0.0023	0.945

Table 5. Fairness–efficacy balance under different sensitive attributes for RQ-4. Results are averaged over 5-fold cross-validation. Metrics with \uparrow indicate higher is better, while metrics with \downarrow indicate lower is better. *Note: While some methods perform better on individual F1 or EO Gap metrics, CurvFed attains the highest FATE score, reflecting the overall fairness–utility balance*

6 Feasibility Study

In this section, we conduct a rigorous empirical study of *CurvFed* in real-world settings. We systematically evaluate its deployment feasibility (Section 6.1) with additional runtime benchmarking/overhead analysis detailed in Appendix B. Furthermore, we discuss sensitivity to key factors (Sections 6.2 and 6.2.4), and conclude with an ablation study that substantiates the effectiveness of the core design choices (Section 6.3).

6.1 Assessing Real-World Deployment Feasibility of *CurvFed*’s Modules

To validate *CurvFed*’s feasibility on heterogeneous edge hardware, we conducted a comprehensive runtime evaluation using a physical FL testbed. Our setup mapped the 48 participants from the Stress Sensing dataset



Fig. 2. Experimental setup and client distribution for real-world FL evaluation using heterogeneous edge devices.

(Section 5.1)—augmented with two randomized duplicates to standardize the cohort size at $N = 50$ clients—to a heterogeneous cluster of six edge devices. This cluster included two Google Pixel 6 smartphones, a Raspberry Pi 5, an NVIDIA Jetson Nano, and two Intel i5-14600T desktops (Fig. 2). Each device executed distinct, isolated client workloads to simulate realistic deployment conditions, training local models and exchanging updates with a central server via Google Cloud APIs authenticated through PyDrive. The following subsections analyze the computational overhead incurred by this specific 50-client configuration, first examining the client-side training costs and subsequently evaluating the server-side aggregation performance.

6.1.1 Client-Side Computational Overhead Analysis: We focus first on the local training costs incurred by the heterogeneous edge devices. Table 6 breaks down the computational overhead of our approach compared to standard (*Benign*) FL training and an ablation variation without the SAM optimizer, just using Equation 11. The results confirm that **CurvFed** imposes minimal overhead, remaining well within the operational limits of modern edge platforms.

- **Training Latency:** The results from Table 6 show that, although curvature regularization ($\lambda(F_{\text{client}})$ penalty) and SAM introduce additional gradient computations, the resulting latency increase is modest. Even on resource-constrained devices such as the Jetson Nano, average per-client training time remains below 0.8s. On more capable hardware, our complete **CurvFed** module shows average-per-client latency of about ($\approx 0.2s$). The overhead of **CurvFed** compared to the benign variant across devices remains small $\approx 0.2 - 0.4s$ and about $\approx 0.1 - 0.3s$ when compared to the ablation variant without SAM, rendering it insignificant relative to typical network communication delays (Appendix Table 17)
- **Resource Utilization:** Memory usage remained stable, with **CurvFed** incurring $< 1\%$ additional RAM overhead compared to the others. CPU utilization varied by architecture (higher on Raspberry Pi, lower on Desktop) but stayed within safe operating ranges, avoiding utilization spikes that could degrade device stability or battery life.
- **Communication Stability:** Upload latencies were consistent across all methods ($\approx 1.6-2.9s$), confirming that our optimization objective does not inflate model checkpoints or hinder transmission reliability.

6.1.2 Server-Side Computational Overhead Analysis: To validate the deployment feasibility of **CurvFed** on standard aggregation servers [60], we profiled the computational cost of our server level design choices, i.e., Stochastic Weight Averaging (SWA) update step relative to the standard Federated Averaging (FedAvg) aggregation. It is important to note that **CurvFed**'s sharpness-aware weighted aggregation scheme (Equation 12) follows the same aggregation procedure as FedAvg, differing only in the choice of weighting coefficients. These weights

Client Assignments	Device	Method	Avg Training Time (s) \pm std	Avg. Memory (MB)	Avg. Train Usage (%)	Avg. Upload Time (s)
Client 1-8	Google Pixel 6	Benign Training	0.28 \pm 0.02	292.78	27.38	2.6402
		Eq 11	0.42 \pm 0.16	296.19	26.67	2.3620
		CurvFed	0.43 \pm 0.05	295.64	27.40	2.3574
Client 9-16	Jetson Nano	Benign Training	0.25 \pm 0.10	321.07	3.20	1.76
		Eq 11	0.35 \pm 0.12	321.59	3.90	1.8248
		CurvFed	0.77 \pm 0.21	321.08	5.45	1.6292
Client 17-24	Google Pixel 6	Benign Training	0.30 \pm 0.02	291.99	27.48	2.2517
		Eq 11	0.38 \pm 0.05	296.49	27.22	2.2923
		CurvFed	0.47 \pm 0.06	296.09	27.66	2.9414
Client 25-32	Intel i5-14600T	Benign Training	0.12 \pm 0.02	285.64	2.64	2.0143
		Eq 11	0.24 \pm 0.02	286.55	2.73	1.9582
		CurvFed	0.27 \pm 0.02	286.96	3.02	2.0142
Client 33-40	Raspberry Pi	Benign Training	0.24 \pm 0.04	312.65	42.7	1.9864
		Eq 11	0.39 \pm 0.09	314.57	42.50	1.9634
		CurvFed	0.37 \pm 0.02	314.65	42.69	2.0028
Client 40-50	Intel i5-14600T	Benign Training	0.15 \pm 0.06	285.65	2.64	1.937
		Eq 11	0.30 \pm 0.06	286.55	3.29	1.9204
		CurvFed	0.26 \pm 0.02	286.95	2.71	1.9586

Table 6. Client side training statistics (averaged) from the real-world FL deployment. Metrics include training time (mean \pm std), Process RSS memory (MB), average CPU utilization (%), and model upload latency (s).

encode client curvature and utility information (W^r); consequently, the server-side runtime overhead remains identical to FedAvg. We utilized a high-performance workstation equipped with an AMD Ryzen 9 7950X CPU and an NVIDIA GeForce RTX 4090 GPU to simulate a realistic server environment handling 50 concurrent client updates. Table 7 summarizes the Time, Memory, and Hardware Utilization for aggregating 50 client models (FedAvg) versus updating the global SWA model.

Our profiling reveals that the SWA update step incurs *negligible computational overhead* compared to the FedAvg aggregation.

- **Aggregation (FedAvg):** The standard FedAvg aggregation of 50 client models requires iterating through all client parameters, resulting in a processing time of approximately 1ms on CPU and 5ms on GPU. The slightly higher latency on the GPU is attributed to the PCIe data transfer[82] overhead dominating the arithmetic operations for these model sizes [60].
- **SWA Update:** In contrast, the SWA update involves a simple weighted moving average between only two sets of parameters. This operation is mathematically $O(1)$ (Line 21 in Algorithm 1), whereas FedAvg is $O(K)$ relative to the number of clients K (Line 18 in Algorithm 1). Consequently, the SWA update time was unmeasurable (< 1 ms). The increased GPU utilization (32.0%) confirms better efficiency: unlike FedAvg, which frequently leaves the GPU idle to wait for loading client model, SWA performs continuous computation on data already in memory [88].

These results demonstrate that integrating SWA into the server-side workflow does not introduce *any latency overhead*. The computational bottleneck remains the aggregation of client updates and network communication, not the SWA optimization. This justifies our design choice to leverage SWA for improving generalization [34] without compromising the real-time constraints of ubiquitous computing environments.

6.1.3 Communication Overhead: We compare *CurvFed*'s communication cost with FL baselines: Fedavg, KD-Fedavg and FedSWA approaches exchange 34.38MB (WIDAR) and 0.042MB (Stress Sensing) per round. As

Platform	Method	Time (s)	Peak Mem (MB)	CPU (%)	GPU (%)
CPU	FedAvg	0.001	511.477	3.873	–
	SWA Update	≈ 0.000	512.477	5.300	–
GPU	FedAvg	0.005	638.742	4.205	26.892
	SWA Update	≈ 0.000	638.742	2.600	32.000

Table 7. Aggregation Performance Comparison (Avg 50 Clients). **CPU**: AMD Ryzen 9 7950X 16-Core Processor, **GPU**: NVIDIA GeForce RTX 4090

overhead, *CurvFed* adds only 8 bytes for sharpness-aware aggregation, while FedSRCVaR adds 4 bytes for a risk threshold—both negligible relative to their fairness benefits.

6.2 Sensitivity Analysis

In this section, we explore the performance and practicality of *CurvFed* under the following real-world scenarios:

- (1) **Effect of Ordered Sampling on FL Performance**
- (2) **Effect of Subsampling Local Labeled Data and Clients on Global Fairness**
- (3) **Impact of Random Client Participation on Fairness Across Models**

Here, we focus on the WIDAR and Stress Sensing datasets using *sex* as the sensitive attribute. They were chosen for their contrasting modalities: WIDAR is uni-modal, while Stress Sensing is multi-modal. While FedSAM and FedSWA were previously compared for benign generalization, they are excluded here to emphasize fairness-oriented baselines: FedAvg serves as the primary benign baseline, and KD-FedAvg and FedSRCVaR serve as FWD FL baselines.

6.2.1 Effect of Ordered Sampling on FL Performance: Human-sensing data often contains strong temporal dependencies [51, 57], making it important to preserve data order during local training [55, 58]. It also mimics real-world FL deployments [89]. To reflect this, we evaluate FL performance using an ordered 80:20 train-test split without shuffling. As shown in Table 8, *CurvFed* achieves the best fairness–utility tradeoff, reducing the EO gap and achieving the highest F1 and FATE scores, demonstrating its effectiveness in temporally structured FL settings.

Dataset	Model	F1 Score ↑	EO Gap ↓	FATE Score $\times 10^{-1}$ ↑
WIDAR	FedAvg	0.8570	0.4629	0.0000
	FedSRCVaR	0.7676	0.4002	0.311
	KD-FedAvg	0.8135	0.4069	0.701
	<i>CurvFed</i>	0.7488	0.3452	1.280
Stress Sensing	FedAvg	0.7482	0.4000	0.0000
	FedSRCVaR	0.6989	0.3633	0.259
	KD-FedAvg	0.7326	0.3633	0.709
	<i>CurvFed</i>	0.7693	0.2938	2.935

Table 8. Performance comparison under ordered 80:20 train–test splits. *CurvFed* achieves the lowest EO Gap and highest FATE score, indicating improved fairness and a superior fairness–utility trade-off, while maintaining competitive F1 performance.

6.2.2 Effect of Subsampling of Local Labeled Data and Clients on Global Fairness: In real-world edge deployments, clients often operate under resource constraints, leading to limited local data and sporadic client availability [46]. To simulate this, we evaluate *CurvFed* under (i) varying local training data availability (20%, 50%, 90%), and (ii) fluctuating client participation per round (3, 5, 7 clients), with a fixed 20% test set.

As shown in Figs. 3 and 4, *CurvFed* consistently demonstrates competitive or superior performance in terms of both fairness (lower EO gap) and utility (higher FATE score) across the WIDAR and Stress Sensing datasets. Notably, in low-data regimes (e.g., 20%), *CurvFed* maintains a clear advantage over FedAvg and KD, while FedSRCVaR occasionally achieves lower EO gaps but with significant sacrifices in FATE scores—especially

evident in the WIDAR dataset with 3 and 5 clients. Furthermore, CurvFed’s performance stabilizes with $\geq 50\%$ data, suggesting robustness even with moderate training data. In client subsampling scenarios, CurvFed maintains the best fairness-utility balance across different client counts, indicating its suitability for dynamic, resource-constrained FL deployments.

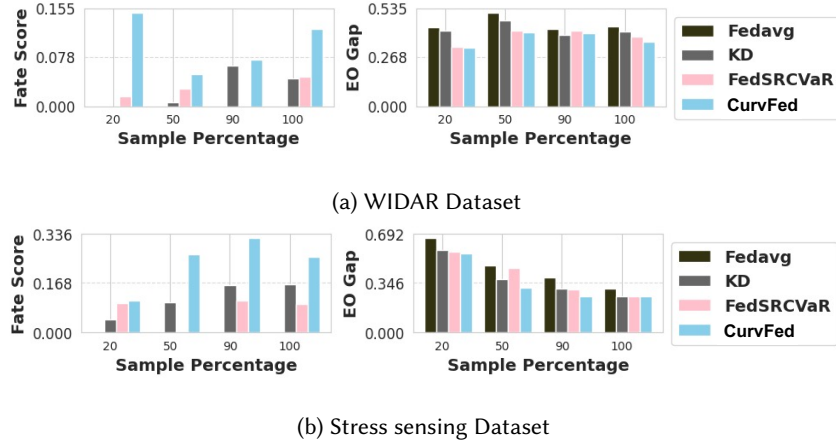


Fig. 3. Impact of limited local data availability (20%, 50%, 90%) on fairness and utility in FL. The **left** subplots report the FATE score (higher is better), while the **right** subplots report the EO gap (lower is better). Results are shown for the (a) WIDAR dataset (top row) and (b) Stress Sensing dataset (bottom row). CurvFed consistently achieves higher FATE scores and lower EO gaps than baseline methods, demonstrating a superior fairness–utility trade-off under limited local data.

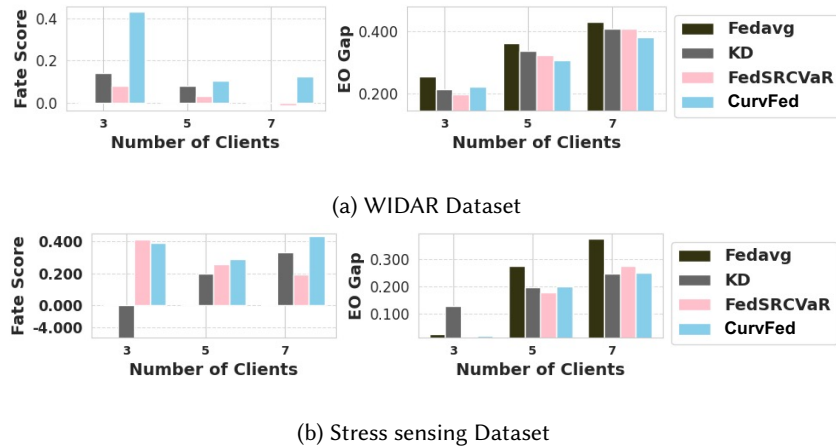


Fig. 4. Impact of client participation subsampling (3 or 5 or 7 clients per round) on fairness–utility trade-off. The **left** subplots report the FATE score (higher is better), while the **right** subplots report the EO gap (lower is better). Results are shown for the (a) WIDAR dataset (top row) and (b) Stress Sensing dataset (bottom row). CurvFed consistently achieves the highest FATE scores and lower EO gaps than baseline methods, demonstrating improved fairness–utility trade-offs under client subsampling.

6.2.3 Impact of Random Client Participation on Fairness: In real-world FL deployments, especially in human-sensing applications, client availability is often inconsistent due to network instability and device constraints [54]. Unlike idealized settings with fixed clients per round, edge devices may randomly join or drop out during training. We simulate this, where clients were independently sampled using Bernoulli sampling with each client having a random probability (ranging from 0.1 to 0.9) of getting selected, introducing realistic variations in both the number and identity of participating clients.

Despite this variability, *CurvFed* consistently achieves the best fairness–accuracy tradeoff, achieving the highest FATE scores—while also attaining the lowest EO gaps, as shown in Fig. 5. While FedSRCVaR sometimes matches fairness, it sacrifices accuracy, and KD-FedAvg shows unstable results. These results demonstrate *CurvFed*'s robustness to client variability in practical FL deployments.

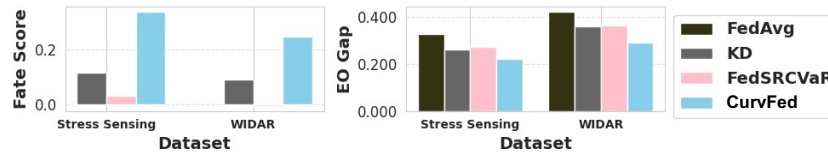


Fig. 5. Experiment on real-world FL evaluation simulating an inconsistent number of clients in each round. The **left** subplots report the FATE score (higher is better), while the **right** subplots report the EO gap (lower is better). *CurvFed* consistently attains higher FATE scores and lower EO gaps across datasets, indicating improved fairness–utility trade-offs.

6.2.4 Sensitivity to the Weighting Parameter α . We study the sensitivity of *CurvFed* to the weighting parameter α by examining its effect on classification performance (F1 score), fairness (EO Gap), and their combined trade-off measured by the FATE score. The parameter α controls the relative weighting of the components in the client-side optimization objective (Equation 11), and its impact is therefore evaluated empirically.

We performed a grid search over $\alpha \in \{0.1, 0.2, \dots, 0.8, 0.92, 0.95\}$ and report the corresponding F1 score, EO Gap, and FATE score. As shown in Figure 6, varying α leads to different performance–fairness profiles across datasets. We selected dataset-specific values of α corresponding to regions where the FATE score is comparatively high and both F1 score and EO Gap remain stable. In particular, $\alpha = 0.8$ is selected for Percept-R, whereas $\alpha = 0.92$ is used for Stress Sensing, WIDAR, and HugaDB datasets. These choices reflect operating points that provide a balanced trade-off between utility and fairness as observed in the empirical results.

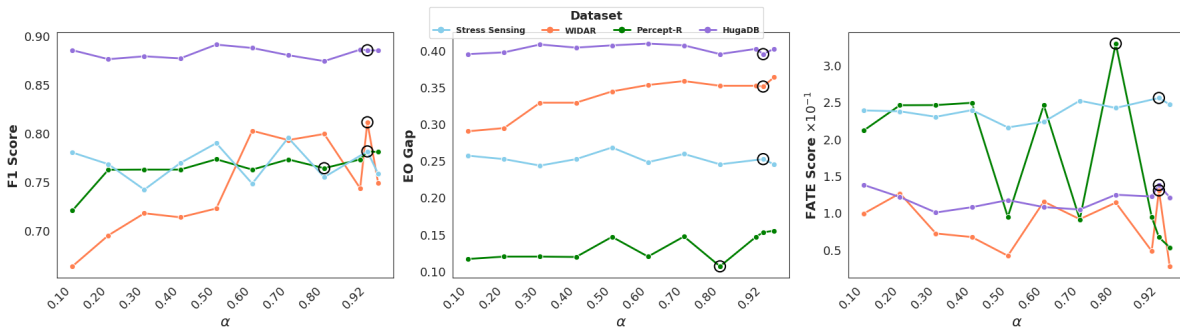


Fig. 6. Impact of the weighting parameter α on (left) F1 score, (middle) EO gap, and (right) FATE score across datasets. Highlighted points denote the selected α values obtained via grid search, which balance higher F1 score, lower EO gap, and higher FATE score.

6.3 Ablation Study

To rigorously evaluate the architectural decisions underpinning *CurvFed*, we conducted a component-wise ablation study across all datasets using 5-fold cross-validation. The goal was to disentangle both the individual and joint contributions of local curvature regularization and global sharpness-aware aggregation to achieving Fairness Without Demographics (FWD), as well as to clarify the roles of SAM in local client training and SWA in server-side aggregation. Table 9 reports the cross-validated performance across twelve distinct configurations for the PERCEPT-R dataset, enabling an analysis of the trade-offs between model utility (F1 score) and equity (EO Gap). Results for the remaining datasets are provided in Appendix C.1.

#	Dataset	Client-Side Training	Aggregation Strategy	F1 Score Mean \pm Std (\uparrow)	EO Gap Mean \pm Std (\downarrow)	FATE $\times 10^{-1}$ Mean Score (\uparrow)
1	PERCEPT-R	Benign	Fedavg	0.7774 \pm 0.0029	0.1626 \pm 0.0060	0.000
2		SAM	Fedavg	0.7784 \pm 0.0030	0.1509 \pm 0.0125	0.732
3		SAM	Fedswa	0.7726 \pm 0.0026	0.1305 \pm 0.0139	1.914
4		SAM+(Eq11)	Fedswa	0.7727 \pm 0.0025	0.1312 \pm 0.0143	1.871
5		(Eq11)	Fedavg	0.7474 \pm 0.0023	0.1291 \pm 0.0050	1.734
6		(Eq11)	(Eq12)	0.7866 \pm 0.0022	0.1589 \pm 0.0131	0.287
7		SAM+(Eq11)	(Eq12)	0.7793 \pm 0.0026	0.1483 \pm 0.0119	0.905
8		(Eq11)	Sharpness Aware aggregation	0.7736 \pm 0.0025	0.1514 \pm 0.0125	0.642
9		SAM	Fedswa+S(L) (Eq12* partial)	0.7664 \pm 0.0100	0.1324 \pm 0.0280	1.717
10		SAM	Fedswa+S(T) (Eq12* partial)	0.7699 \pm 0.0037	0.1288 \pm 0.0207	1.987
11		SAM	Sharpness Aware aggregation	0.7662 \pm 0.0101	0.1318 \pm 0.0293	1.753
12		SAM+(Eq11)	Sharpness Aware aggregation	0.7642 \pm 0.0030	0.1062 \pm 0.0119	3.296

Table 9. Ablation of *CurvFed*'s design choices on the PERCEPT-R dataset. Results are averaged over 5-fold cross-validation. **Client-Side Training** indicates the optimization or regularization applied locally at each client. **Aggregation Strategy** specifies the server-side model aggregation rule. Unless explicitly stated, each row applies *only* the listed client-side or aggregation component, with no additional modifications. Metrics with \uparrow indicate higher is better, while \downarrow indicates lower is better. Best values for F1, EO Gap, and FATE are bolded. Rows are numbered for reference in the text.

This study systematically isolates and evaluates the independent contributions of three key components: (1) the *Local curvature constraints* during client-side training, (2) *CurvFed*'s *sharpness-aware aggregation strategy* (the sharpness-aware weighting scheme W^r in Equation 12 combined with SWA), and (3) synergistic effect arising from *integrating all components* within the full *CurvFed* framework.

6.3.1 The Efficacy of Local Curvature Constraints. Our approach is based on the idea that local model sharpness correlates with biased decision boundaries. We validated this by applying the FIM penalty ($\lambda(F_{client})$) during local training, i.e., following Equation 11, while maintaining a standard FedAvg aggregation (Row 5). Results from this isolation demonstrates that *restricting the local search space to flatter regions inherently mitigates bias*: the EO Gap decreased by **20.60%** compared to the benign baseline (Row 1). While this constraint induced a modest drop in F1 score ($\approx 3\%$), it provides empirical evidence that individual clients can contribute to global fairness through geometric regularization alone, even without server-side coordination.

To further disentangle the contribution of client-side curvature constraints from server-side sharpness-aware aggregation within the *CurvFed* design, we evaluated an additional variant in which the sharpness-aware weighting scheme W^r (Equation 12) was removed, while all other *CurvFed* components were preserved (Row 4). This configuration achieved a lower EO Gap (**19.31%** reduction) and comparable F1 score relative to the benign baseline (Row 1), but underperformed compared to the full *CurvFed* framework (Row 12).

Overall, these findings confirm that local curvature constraints independently promote fairness gains; however, their full potential is realized only when combined with server-side sharpness-aware aggregation, highlighting the complementary and synergistic design of the complete *CurvFed* framework.

6.3.2 Sharpness-Awareness at the Aggregator. We next examined the role of the server in mitigating biased client updates. To isolate the effect of our Sharpness-Aware Aggregation (the sharpness-aware weighting scheme W^r in Equation 12 combined with SWA), we removed the local curvature constraint (Equation 11) from the *CurvFed* framework (Row 11) and compared it against clients trained with SAM while the server used standard FedAvg (Row 2)—keeping client-side training consistent across settings. Isolated Sharpness-Aware Aggregation of *CurvFed* reduced the EO Gap by **12.65%** relative to the baseline (Row 2). This suggests that simply averaging locally flat models (SAM+FedAvg; where SAM promotes flatter minima) is insufficient; the aggregation mechanism itself must account for the sharpness of the incoming updates to prevent the re-introduction of sharp, biased minima during the global update step.

6.3.3 Navigating the Fairness-Utility Tension. The ablation results illustrate the distinct roles of aggregation and local optimization in balancing the accuracy-fairness trade-off. Notably, Row 6—which combines applying the FIM penalty ($\lambda(F_{client})$) during local training, i.e., following Equation 11, with the sharpness-aware weighting scheme W^r in Equation 12—achieved the *highest absolute F1 score* (0.7866) of all configurations. This result confirms that our curvature-aware aggregation strategy is highly effective at identifying and promoting stable, high-performing models. However, this configuration yielded a modest FATE score (0.287) with a small EO Gap reduction than the benign baseline (Row 1). In contrast, the full *CurvFed* integration (Row 12) accepts a minor utility trade-off (1.32% lower F1 than benign baseline) to secure a dramatic **34.66% reduction** in EO Gap compared to Benign Fedavg (Row 1). Consequently, *CurvFed* achieves the highest FATE score (3.296) among all methods. These findings suggest that applying curvature constraints alone—via FIM regularization at both the client and server levels—can make optimization more challenging. In contrast, incorporating SAM and SWA at the client and server, respectively, facilitates smoother optimization dynamics, enabling the model to reach a more favorable fairness-utility trade-off and effectively address the FWD objective.

7 Empirical Justification

While Section 5 confirms the effectiveness of *CurvFed*, this section offers an empirical justification of *why and how* it works. Specifically, we empirically evaluate whether the observed outcomes support the propositions introduced in Section 3.2, which hypothesize the mechanisms through which CurvFed improves fairness and performance in the absence of sensitive attributes. Each of the following subsections corresponds to one of the three propositions and presents analysis and visualizations using the WIDAR and stress sensing datasets.

(Validation of P1) Alignment between FIM and Hessian top eigenvalue: Fig. 7 illustrates the relationship between communication rounds and test-set model performance in terms of the FATE Score, F1 Score, and Loss Landscape, for the Stress Sensing dataset and WIDAR dataset. We utilized FATE score as our selection criterion for the best global model highlighted in yellow, corresponding to round 20.

Fig. 8 shows the mean per-person top eigenvalues of the Hessian and FIM for the Stress Sensing in Fig. 8 (a) and WIDAR dataset in Fig. 8 (b). Notably, the graph traits for both FIM and Hessian are similar, and lowest in our optimal selected round (20), providing empirical justification for *proposition 1*.

(Validation of P2) Minimizing the FIM Top Eigenvalue Reduces group Curvature Disparity: To evaluate whether FL training aligns with proposition 2 discussed in Section 3.2, we analyze the difference in curvature metrics across known sensitive attribute groups. Table 10 reports the difference in the top eigenvalues (λ) of the FIM and Hessian matrix for the sensitive attribute *sex* across two distributions, D_{male}^{sex} and D_{female}^{sex} along with the FATE scores for the WIDAR and Stress sensing datasets.

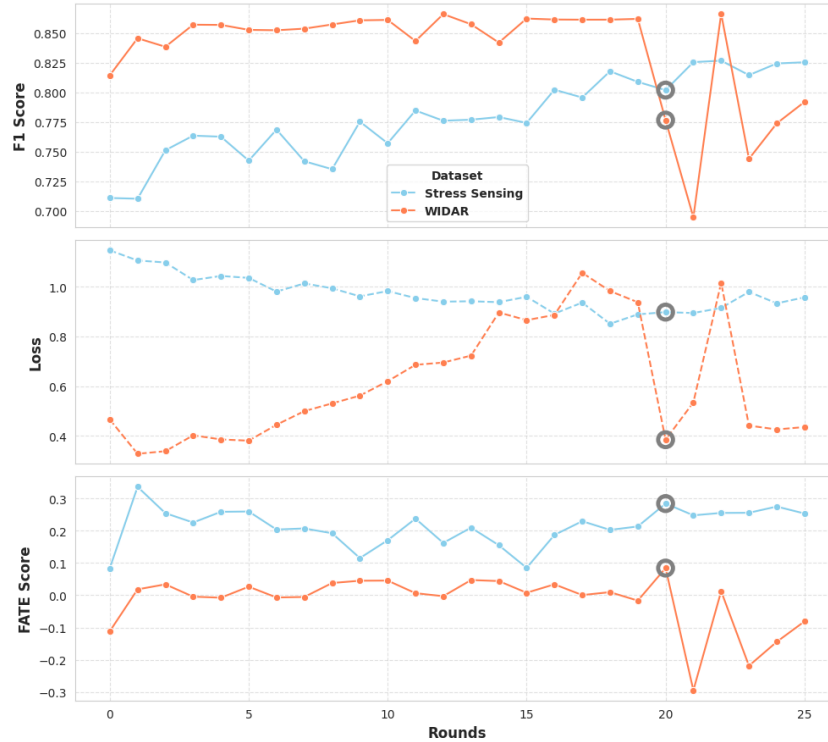


Fig. 7. Evolution of F1 score (top), loss (middle), and FATE score (bottom) across communication rounds for CurvFed on the Stress Sensing and WIDAR datasets. Both datasets exhibit similar convergence trends, with F1 and FATE scores stabilizing as loss decreases. The highlighted round corresponds to the point where both loss and F1 converge, and it also aligns with a stable or improved FATE score, indicating a balanced trade-off

Global Trends: FedSAM and FedSWA reduce curvature disparity via implicit sharpness minimization at the client and server levels, respectively. While this results in moderate gains in both curvature alignment and FATE scores, **CurvFed** consistently outperforms them in curvature alignment and FATE scores, confirming the superior effectiveness of explicit FIM-based sharpness regularization.

Client-Level Trends: Does CurvFed Reduce group-wise Disparity Locally? To examine whether global fairness trends extend to individual clients, we visualize group-wise FIM eigenvalues for randomly selected clients from the Stress Sensing dataset (see Fig. 9). We analyze changes across sensitive attributes such as *sex* and *handedness* before and after local training.

The visualizations show that reducing the top eigenvalue of the FIM not only lowers overall curvature but also reduces disparity between groups at the client level—supporting our *proposition 2*.

(Validation of P3) Sharpness-Aware Aggregation Reduces Variance in Excessive Loss Across Clients: To verify whether **CurvFed** indeed upholds this proposition, we visualized the $\lambda(F_{client})$ and classification loss among single-person and multi-person clients in FL systems for WIDAR and Stress-Sensing datasets, as shown in Fig. 10. **CurvFed** outperforms other FWD baselines by consistently reducing variance across the excessive loss in the form of ‘reducing variances across the top eigenvalue values $\lambda(F)$ and loss’ across clients. *This visualization confirms proposition 3.*

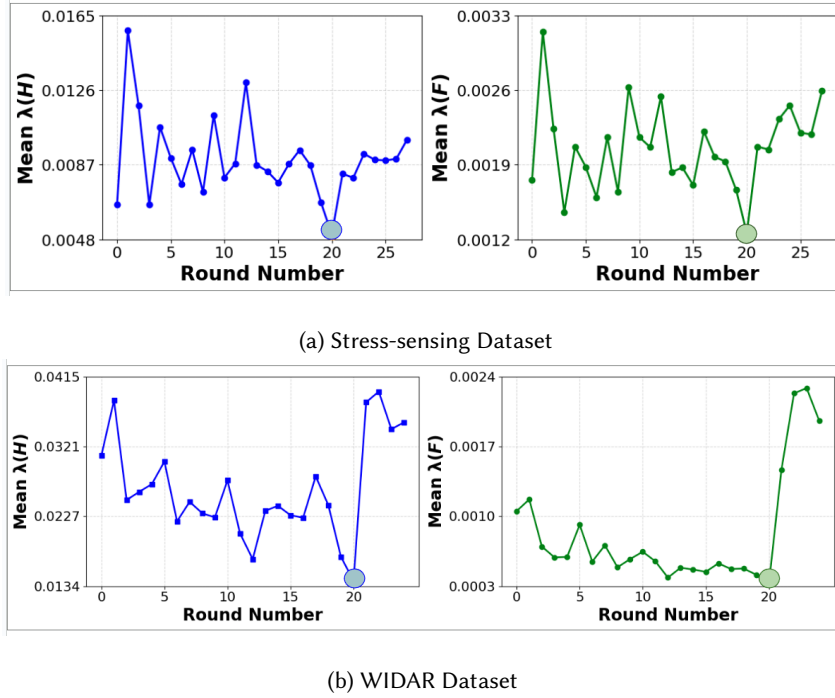


Fig. 8. Mean person-wise top eigenvalues of the Hessian (left) and Fisher (right) matrices across federated learning rounds for the Stress Sensing (top row) and WIDAR (bottom row) datasets. Both datasets exhibit similar decreasing and stabilizing trends, indicating consistent optimization behavior across tasks. Lower eigenvalues correspond to flatter and more stable solutions. The highlighted rounds, selected based on F1 and loss convergence, aligning with minimum eigenvalues.

Dataset	Model	$\Delta\lambda(\mathbf{F}) \downarrow$	$\Delta\lambda(\mathbf{H}) \downarrow$	FATE Score $\times 10^{-1} \uparrow$
WIDAR	Fedavg	0.009	0.061	0.0000
	FedSAM	0.009	0.0365	-0.56
	FedSWA	0.002	0.019	0.33
	FedSRCVaR	0.0015	0.0310	0.160
	KD-Fedavg	0.0022	0.0377	0.122
	CurvFed	0.0007	0.0017	1.233
Stress Sensing	Fedavg	0.03	0.0330	0.0000
	FedSAM	0.019	0.0347	0.812
	FedSWA	0.020	0.0278	0.38
	FedSRCVaR	0.019	0.1446	0.319
	KD-Fedavg	0.021	0.6089	1.645
	CurvFed	0.004	0.0097	2.559

Table 10. Disparity based on ‘Sex’ Across Datasets for Different Models. Metrics with \uparrow indicate higher is better, while metrics with \downarrow indicate lower is better. CurvFed achieves the lowest disparity measures and the highest FATE score across both datasets.

8 Broader Impact and Limitation

This first-of-its-kind paper bridges the gap between fairness and federated learning in human-sensing applications, paving the way for a more equitable and responsible future in decentralized human-sensing, ensuring fair access to technological advancements for all. *Some limitations and future research scopes are discussed below:*

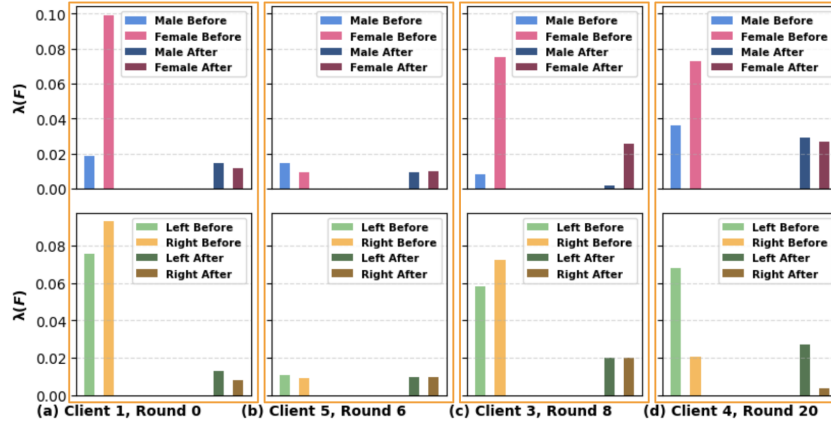
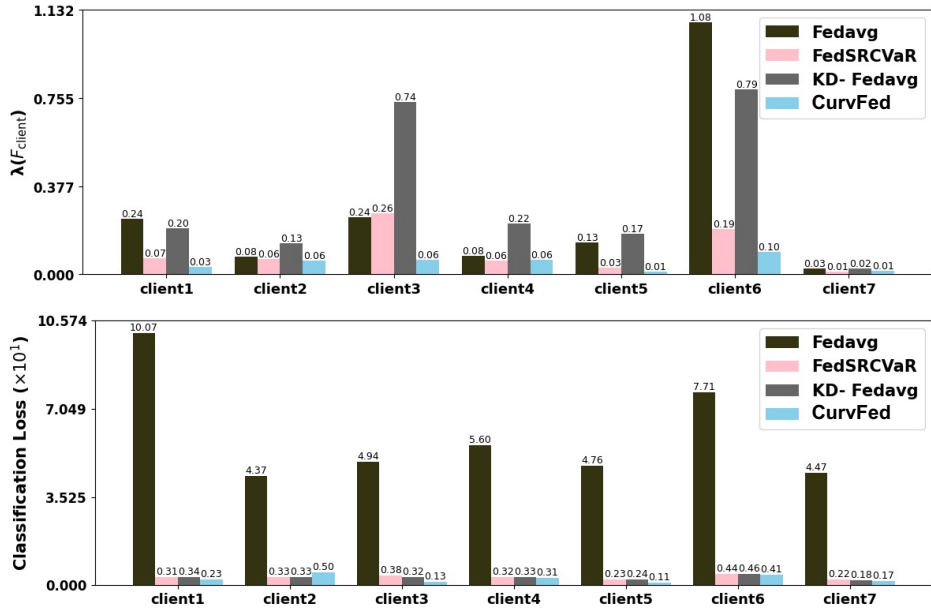
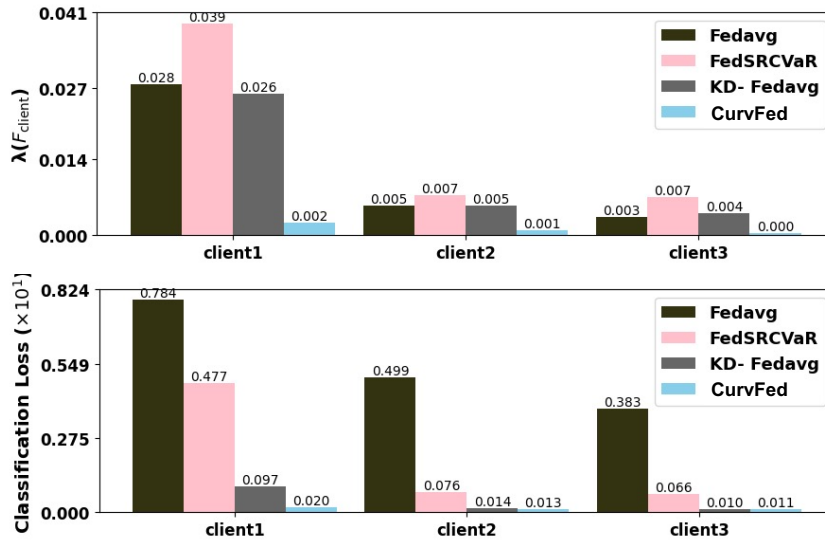


Fig. 9. Top Fisher eigenvalues by sex (top) and hand (bottom) across clients and rounds in the Stress Sensing dataset. Bars labeled “Before” and “After” denote values prior to and following the application of the fairness-aware training. Reduced gaps between groups and lower $\lambda(F)$ and $\lambda(H)$ values after training indicate decreased group-level disparity and improved optimization stability.

- Achieving fairness in FL systems requires attaining a balance between fairness and model performance [27]. The quest to ensure fairness for individual clients often results in reduced performance across the board, an issue highlighted in literature [4, 23, 84, 100]. Although *CurvFed* demonstrates significant effectiveness in achieving this balance, as discussed in Section 5.3, **RQ-3**, it exhibits minor performance degradation in the WIDAR and Stress sensing dataset for single-person clients. This could be attributed to our aggregation scheme, outlined in Section 4.1 Equation 12, which equally weighs low error rates and lower maximal uncertainty, thus limiting the ability to balance accuracy and fairness when dealing with single-person clients. The issue could be resolved by introducing a hyperparameter as the weighting factor.
- Recent studies have explored the relationship between fairness and privacy in machine learning, often treating them as competing metrics [80, 102]. While this work has focused on fairness in FL, extending the investigation to explore the interplay between fairness and privacy in FL would be an important direction for future research.
- A limitation of our study is the experimental scale, constrained by the lack of large-scale human-sensing datasets with sensitive attributes. While prior (non-human-centric) FL fairness works often evaluate on a larger number of clients, such datasets remain scarce in the human sensing domain [96]. Even recent large-scale datasets like GLOBEM [91] do not release demographic or other sensitive information needed for fairness evaluation. This gap has also been discussed in recent survey studies within the ubiquitous sensing community [95, 97].
- Like many Rawlsian or min-max fairness approaches [30, 42], *CurvFed* promotes equity by aligning loss landscape curvatures across clients, which prioritizes worst-case (or underrepresented) groups. This strategy can occasionally come at the expense of performance in majority groups, a trade-off that has also been reported in other fairness-driven FL methods [20, 62, 65]. While this reflects a broader property of parity-based optimization [26, 64] rather than a limitation of *CurvFed* itself, it highlights an important avenue for future research: designing FWD mechanisms that uplift the worst-off groups without diminishing performance for others, thereby moving toward Pareto-improving fairness [63, 98].



(a) Stress Sensing Dataset



(b) WIDAR Dataset

Fig. 10. Client-wise comparison of the maximum Fisher eigenvalue $\lambda(F_{client})$ (top) and classification loss (bottom) across federated learning models on the Stress Sensing (top row) and WIDAR (bottom row) datasets. Lower values in both metrics indicate more stable client updates and reduced client-level disparity. CurvFed consistently achieves lower Fisher eigenvalues and lower classification loss across clients, demonstrating improved optimization stability and reduced fairness-related client heterogeneity

9 Conclusion

This paper presents **CurvFed**, a novel fairness-enhancing strategy for FL that introduces sharpness-aware regularization during local training and aggregation. Unlike existing methods, **CurvFed** is theoretically grounded and operates without access to sensitive or bias-inducing attributes, thereby preserving FL’s core privacy principles. Extensive evaluations—including a live real-world deployment on heterogeneous, resource-constrained edge devices—demonstrate **CurvFed**’s effectiveness in achieving a strong fairness–performance trade-off across diverse human-sensing applications, even under single- or multi-user scenarios with multiple unknown bias sources. Ablation studies and empirical justifications further validate that leveraging loss-landscape sharpness is key to improving fairness. Overall, **CurvFed** offers a practical and privacy-respecting path forward for equitable FL in real-world human-sensing systems.

References

- [1] Annie Abay, Yi Zhou, Nathalie Baracaldo, Shashank Rajamoni, Ebube Chuba, and Heiko Ludwig. 2020. Mitigating bias in federated learning. *arXiv preprint arXiv:2012.02447* (2020). doi:10.48550/arXiv.2012.02447
- [2] Qamar Abbas, Khalid Mahmood Malik, Abdul Khader Jilani Saudagar, and Muhammad Badruddin Khan. 2023. Context-aggregator: An approach of loss-and class imbalance-aware aggregation in federated learning. *Computers in Biology and Medicine* 163 (2023), 107167. doi:10.1016/j.combiomed.2023.107167
- [3] Takuya Akiba, Shotaro Sano, Toshihiko Yanase, Takeru Ohta, and Masanori Koyama. 2019. Optuna: A next-generation hyperparameter optimization framework. In *Proceedings of the 25th ACM SIGKDD international conference on knowledge discovery & data mining*. 2623–2631. doi:10.48550/arXiv.1907.10902
- [4] Md Tanvir Al Amin, Tarek Abdelzaher, Dong Wang, and Boleslaw Szymanski. 2014. Crowd-sensing with polarized sources. In *2014 IEEE International Conference on Distributed Computing in Sensor Systems*. IEEE, 67–74. doi:10.1109/DCOSS.2014.23
- [5] Alessandra Arcuri and Giuseppe Dari-Mattiacci. 2010. Centralization versus decentralization as a risk-return trade-off. *The Journal of Law and Economics* 53, 2 (2010), 359–378. doi:10.1086/599623
- [6] Nina R Benway, Jonathan Preston, Elaine Hitchcock, Asif Salekin, Harshit Sharma, and Tara McAllister. 2022. PERCEPT-R: An open-access American English child/clinical speech corpus specialized for the audio classification of /ɪ/. (2022). doi:10.21437/Interspeech.2022-10785
- [7] Stephen P Boyd and Lieven Vandenbergh. 2004. *Convex optimization*. Cambridge university press. doi:10.1007/978-1-4614-5257-7_6
- [8] Debora Caldarola, Barbara Caputo, and Marco Ciccone. 2022. Improving generalization in federated learning by seeking flat minima. In *European Conference on Computer Vision*. Springer, 654–672. doi:10.48550/arXiv.2203.11834
- [9] Alessandro Castelnovo, Riccardo Crupi, Greta Greco, Daniele Regoli, Ilaria Giuseppina Penco, and Andrea Claudio Cosentini. 2022. A clarification of the nuances in the fairness metrics landscape. *Scientific Reports* 12, 1 (2022), 4209. doi:10.1038/s41598-022-07939-1
- [10] Junyi Chai, Taekui Jang, and Xiaoqian Wang. 2022. Fairness without demographics through knowledge distillation. *Advances in Neural Information Processing Systems* 35 (2022), 19152–19164. <https://openreview.net/forum?id=8gjwWnN5pfy>
- [11] Huiqiang Chen, Tianqing Zhu, Tao Zhang, Wanlei Zhou, and Philip S Yu. 2023. Privacy and Fairness in Federated Learning: on the Perspective of Trade-off. *Comput. Surveys* (2023). doi:10.48550/arXiv.2306.14123
- [12] Roman Chereshnev and Attila Kertész-Farkas. 2018. Hugadb: Human gait database for activity recognition from wearable inertial sensor networks. In *Analysis of Images, Social Networks and Texts: 6th International Conference, AIST 2017, Moscow, Russia, July 27–29, 2017, Revised Selected Papers 6*. Springer, 131–141. doi:10.48550/arXiv.1705.08506
- [13] Ching-Hao Chiu, Yu-Jen Chen, Yawen Wu, Yiyu Shi, and Tsung-Yi Ho. 2024. Achieve fairness without demographics for dermatological disease diagnosis. *Medical Image Analysis* 95 (2024), 103188. doi:10.1016/j.media.2024.103188
- [14] Andrew Cotter, Maya Gupta, Heinrich Jiang, Nathan Srebro, Karthik Sridharan, Serena Wang, Blake Woodworth, and Seungil You. 2018. Training fairness-constrained classifiers to generalize. In *ICML 2018 workshop: “fairness, accountability, and transparency in machine learning (FAT/ML)*. doi:10.48550/arXiv.1807.00028
- [15] Sen Cui, Weishen Pan, Jian Liang, Changshui Zhang, and Fei Wang. 2021. Addressing algorithmic disparity and performance inconsistency in federated learning. *Advances in Neural Information Processing Systems* 34 (2021), 26091–26102. doi:10.48550/arXiv.2108.08435
- [16] Yann N Dauphin, Atish Agarwala, and Hossein Mobahi. 2024. Neglected Hessian component explains mysteries in Sharpness regularization. *arXiv preprint arXiv:2401.10809* (2024). doi:10.48550/arXiv.2401.10809
- [17] Yasmine Djebrouni. 2022. Towards bias mitigation in federated learning. In *16th EuroSys Doctoral Workshop*. <https://hal.science/hal-03639179v1>

- [18] Yasmine Djebrouni, Nawel Benarba, Ousmane Touat, Pasquale De Rosa, Sara Bouchenak, Angela Bonifati, Pascal Felber, Vania Marangozova, and Valerio Schiavoni. 2024. Bias Mitigation in Federated Learning for Edge Computing. *Proceedings of the ACM on Interactive, Mobile, Wearable and Ubiquitous Technologies* 7, 4 (2024), 1–35. doi:10.1145/3631455
- [19] Xin Dong, Shangyu Chen, and Sinno Pan. 2017. Learning to prune deep neural networks via layer-wise optimal brain surgeon. *Advances in neural information processing systems* 30 (2017). doi:10.48550/arXiv.1705.07565
- [20] Wei Du, Depeng Xu, Xintao Wu, and Hanghang Tong. 2021. Fairness-aware agnostic federated learning. In *Proceedings of the 2021 SIAM International Conference on Data Mining (SDM)*. SIAM, 181–189. doi:10.48550/arXiv.2010.05057
- [21] Cynthia Dwork, Moritz Hardt, Toniann Pitassi, Omer Reingold, and Richard Zemel. 2012. Fairness through awareness. In *Proceedings of the 3rd innovations in theoretical computer science conference*. 214–226. doi:10.48550/arXiv.1104.3913
- [22] Daniel A Epstein, Clara Caldeira, Mayara Costa Figueiredo, Xi Lu, Lucas M Silva, Lucretia Williams, Jong Ho Lee, Qingyang Li, Simran Ahuja, Qiu Chen, et al. 2020. Mapping and taking stock of the personal informatics literature. *Proceedings of the ACM on Interactive, Mobile, Wearable and Ubiquitous Technologies* 4, 4 (2020), 1–38. doi:10.1145/3432231
- [23] Yahya H Ezzeldin, Shen Yan, Chaoyang He, Emilio Ferrara, and A Salman Avestimehr. 2023. Fairfed: Enabling group fairness in federated learning. In *Proceedings of the AAAI Conference on Artificial Intelligence*, Vol. 37. 7494–7502. doi:10.1016/j.comnet.2024.110663
- [24] Julien Ferry, Ulrich Aivodji, Sébastien Gams, Marie-José Huguet, and Mohamed Siala. 2023. Improving fairness generalization through a sample-robust optimization method. *Machine Learning* 112, 6 (2023), 2131–2192. doi:10.1007/s10994-022-06191-y
- [25] Pierre Foret, Ariel Kleiner, Hossein Mobahi, and Behnam Neyshabur. 2021. Sharpness-aware Minimization for Efficiently Improving Generalization. In *International Conference on Learning Representations*. <https://openreview.net/forum?id=6Tm1mposlrM>
- [26] James R Foulds and Shimei Pan. 2020. Are Parity-Based Notions of AI Fairness Desirable? *A Quarterly bulletin of the Computer Society of the IEEE Technical Committee on Data Engineering* 43, (4) (2020). doi:10.13016/m2uzsk-datb
- [27] Xiuting Gu, Zhu Tianqing, Jie Li, Tao Zhang, Wei Ren, and Kim-Kwang Raymond Choo. 2022. Privacy, accuracy, and model fairness trade-offs in federated learning. *Computers & Security* 122 (2022), 102907. doi:10.1016/j.cose.2022.102907
- [28] Yongxin Guo, Tao Lin, and Xiaoying Tang. 2021. Towards federated learning on time-evolving heterogeneous data. *arXiv preprint arXiv:2112.13246* (2021). doi:10.48550/arXiv.2112.13246
- [29] Faisal Hamman and Sanghamitra Dutta. 2023. Demystifying Local and Global Fairness Trade-offs in Federated Learning Using Partial Information Decomposition. *arXiv preprint arXiv:2307.11333* (2023).
- [30] Tatsunori Hashimoto, Megha Srivastava, Hongseok Namkoong, and Percy Liang. 2018. Fairness without demographics in repeated loss minimization. In *International Conference on Machine Learning*. PMLR, 1929–1938. doi:10.48550/arXiv.1806.08010
- [31] Sepp Hochreiter and Jürgen Schmidhuber. 1997. Flat minima. *Neural Computation* 9, 1 (1997), 1–42. doi:10.1162/neco.1997.9.1.1
- [32] Roger A Horn and Charles R Johnson. 2012. *Matrix analysis*. Cambridge university press. doi:10.1017/CBO9780511810817
- [33] The White House. 2025. Removing Barriers to American Leadership in Artificial Intelligence. *Executive Order* 23 (2025).
- [34] Pavel Izmailov, Dmitrii Podoprikin, Timur Garipov, Dmitry Vetrov, and Andrew Gordon Wilson. 2018. Averaging weights leads to wider optima and better generalization. *arXiv preprint arXiv:1803.05407* (2018). doi:10.48550/arXiv.1803.05407
- [35] Stanisław Jastrzębski, Zachary Kenton, Nicolas Ballas, Asja Fischer, Yoshua Bengio, and Amos Storkey. 2018. On the relation between the sharpest directions of DNN loss and the SGD step length. *arXiv preprint arXiv:1807.05031* (2018).
- [36] Tonni Das Jui and Pablo Rivas. 2024. Fairness issues, current approaches, and challenges in machine learning models. *International Journal of Machine Learning and Cybernetics* (2024), 1–31. doi:10.1007/s13042-023-02083-2
- [37] Ryo Karakida, Shotaro Akaho, and Shun-ichi Amari. 2019. Universal Statistics of Fisher Information in Deep Neural Networks: Mean Field Approach. In *International Conference on Artificial Intelligence and Statistics (AISTATS)*. 1032–1041. doi:arXiv:1806.01316
- [38] Manjeet Kaur. [n. d.]. *Wireless Sensor Networks: Issues & Challenges*. [n. d.]. doi:10.2139/ssrn.1972636
- [39] Nitish Shirish Keskar, Dheevatsa Mudigere, Jorge Nocedal, Mikhail Smelyanskiy, and Ping Tak Peter Tang. 2017. On Large-Batch Training for Deep Learning: Generalization Gap and Sharp Minima. In *International Conference on Learning Representations (ICLR)*. doi:arXiv:1609.04836
- [40] Koffka Khan, Wayne Goodridge, and Winston Elibox. 2025. A Functional RNA-Based and Curvature-Aware Learning Framework for Federated Optimization. *Neurocomputing* (2025), 131045. doi:10.1016/j.neucom.2025.131045
- [41] Young-Ho Kim, Jae Ho Jeon, Eun Kyoung Choe, Bongshin Lee, KwonHyun Kim, and Jinwook Seo. 2016. TimeAware: Leveraging framing effects to enhance personal productivity. In *Proceedings of the 2016 CHI Conference on Human Factors in Computing Systems*. 272–283. doi:10.1145/2858036.285842
- [42] Preethi Lahoti, Alex Beutel, Jilin Chen, Kang Lee, Flavien Prost, Nithum Thain, Xuezhi Wang, and Ed Chi. 2020. Fairness without demographics through adversarially reweighted learning. *Advances in neural information processing systems* 33 (2020), 728–740. doi:10.48550/arXiv.2006.13114
- [43] Khiem Le, Nhan Luong-Ha, Manh Nguyen-Duc, Danh Le-Phuoc, Cuong Do, and Kok-Seng Wong. 2024. Exploring the practicality of federated learning: A survey towards the communication perspective. *arXiv preprint arXiv:2405.20431* (2024). doi:10.48550/arXiv.2405.20431

- [44] Byung-Kwan Lee, Junho Kim, and Yong Man Ro. 2022. Masking adversarial damage: Finding adversarial saliency for robust and sparse network. In *Proceedings of the IEEE/CVF Conference on Computer Vision and Pattern Recognition*. 15126–15136. doi:10.48550/arXiv.2204.02738
- [45] Hoonyong Lee, Changbum R Ahn, Nakjung Choi, Toseung Kim, and Hyunsoo Lee. 2019. The effects of housing environments on the performance of activity-recognition systems using Wi-Fi channel state information: An exploratory study. *Sensors* 19, 5 (2019), 983. doi:10.3390/s19050983
- [46] Ang Li, Jingwei Sun, Xiao Zeng, Mi Zhang, Hai Li, and Yiran Chen. 2021. Fedmask: Joint computation and communication-efficient personalized federated learning via heterogeneous masking. In *Proceedings of the 19th ACM Conference on Embedded Networked Sensor Systems*. 42–55. doi:10.1145/3485730.3485929
- [47] Chenning Li, Zhichao Cao, and Yunhao Liu. 2021. Deep AI enabled ubiquitous wireless sensing: A survey. *ACM Computing Surveys (CSUR)* 54, 2 (2021), 1–35. doi:10.1145/3436729
- [48] Hao Li, Yiqin Luo, Tianlong Gu, and Liang Chang. 2024. BFFN: A novel balanced feature fusion network for fair facial expression recognition. *Engineering Applications of Artificial Intelligence* 138 (2024), 109277. doi:10.1016/j.engappai.2024.109277
- [49] Hao Li, Zheng Xu, Gavin Taylor, Christoph Studer, and Tom Goldstein. 2018. Visualizing the Loss Landscape of Neural Nets. In *Advances in Neural Information Processing Systems (NeurIPS)*. doi:arXiv:1712.09913
- [50] Jian Li, Tongbao Chen, and Shaohua Teng. 2024. A comprehensive survey on client selection strategies in federated learning. *Computer Networks* (2024), 110663. doi:10.1016/j.comnet.2024.110663
- [51] Mohan Li, Martin Gjoreski, Pietro Barbiero, Gašper Slapničar, Mitja Luštrek, Nicholas D Lane, and Marc Langheinrich. 2025. A Survey on Federated Learning in Human Sensing. *arXiv preprint arXiv:2501.04000* (2025). doi:10.48550/arXiv:2501.04000
- [52] Youpeng Li, Xuyu Wang, and Lingling An. 2023. Hierarchical clustering-based personalized federated learning for robust and fair human activity recognition. *Proceedings of the ACM on Interactive, Mobile, Wearable and Ubiquitous Technologies* 7, 1 (2023), 1–38. doi:10.1145/3580795
- [53] Tengyuan Liang, Tomaso Poggio, Alexander Rakhlin, and James Stokes. 2019. Fisher-Rao Metric, Geometry, and Complexity of Neural Networks. In *The 22nd International Conference on Artificial Intelligence and Statistics*. 888–896. doi:arXiv.1711.01530
- [54] Wei Yang Bryan Lim, Nguyen Cong Luong, Dinh Thai Hoang, Yutao Jiao, Ying-Chang Liang, Qiang Yang, Dusit Niyato, and Chunyan Miao. 2020. Federated learning in mobile edge networks: A comprehensive survey. *IEEE Communications Surveys & Tutorials* 22, 3 (2020), 2031–2063. doi:10.1109/COMST.2020.2986024
- [55] Qingxiang Liu, Sheng Sun, Yuxuan Liang, Jingjing Xue, and Min Liu. 2024. Personalized Federated Learning for Spatio-Temporal Forecasting: A Dual Semantic Alignment-Based Contrastive Approach. (2024). doi:10.48550/arXiv.2404.03702
- [56] Xintong Lu, Yuchao Zhang, Huan Zou, Yilei Liang, Wendong Wang, and Jon Crowcroft. 2023. FedCOM: Efficient Personalized Federated Learning by Finding Your Best Peers. In *Proceedings of the 2nd ACM Workshop on Data Privacy and Federated Learning Technologies for Mobile Edge Network*. 107–112. doi:10.1145/3615593.3615720
- [57] Dimitrios Lymberopoulos, Athanasios Bamis, and Andreas Savvides. 2009. A methodology for extracting temporal properties from sensor network data streams. In *Proceedings of the 7th international conference on Mobile systems, applications, and services*. 193–206. doi:10.1145/1555816.155583
- [58] Afra Mashhadi, Ali Tabaraei, Yuting Zhan, and Reza M Parizi. 2022. An Auditing Framework for Analyzing Fairness of Spatial-Temporal Federated Learning Applications. In *2022 IEEE World AI IoT Congress (AlloT)*. IEEE, 699–707. doi:10.1109/AlloT54504.2022.9817283
- [59] Cameron McCarthy, Nikhilesh Pradhan, Calum Redpath, and Andy Adler. 2016. Validation of the Empatica E4 wristband. In *2016 IEEE EMBS international student conference (ISC)*. IEEE, 1–4. doi:10.1109/EMBSISC.2016.7508621
- [60] Brendan McMahan, Eider Moore, Daniel Ramage, Seth Hampson, and Blaise Aguera y Arcas. 2017. Communication-efficient learning of deep networks from decentralized data. In *Artificial intelligence and statistics*. PMLR, 1273–1282. doi:10.48550/arXiv.1602.05629
- [61] Ninareh Mehrabi, Fred Morstatter, Nripsuta Saxena, Kristina Lerman, and Aram Galstyan. 2021. A survey on bias and fairness in machine learning. *ACM computing surveys (CSUR)* 54, 6 (2021), 1–35. doi:10.1145/3457607
- [62] Mehryar Mohri, Gary Sivek, and Ananda Theertha Suresh. 2019. Agnostic federated learning. In *International Conference on Machine Learning*. PMLR, 4615–4625. doi:10.48550/arXiv.1902.00146
- [63] Rashmi Nagpal, Rasoul Shahsavari, Vaibhav Goyal, and Amar Gupta. 2025. Optimizing fairness and accuracy: a Pareto optimal approach for decision-making. *AI and Ethics* 5, 2 (2025), 1743–1756. doi:10.1007/s43681-024-00508-4
- [64] Kirtan Padh, Diego Antognini, Emma Lejal-Glaude, Boi Faltings, and Claudiu Musat. 2021. Addressing fairness in classification with a model-agnostic multi-objective algorithm. In *Uncertainty in artificial intelligence*. PMLR, 600–609. doi:10.48550/arXiv.2009.04441
- [65] Afroditi Papadaki, Natalia Martinez, Martin Bertran, Guillermo Sapiro, and Miguel Rodrigues. 2022. Minimax demographic group fairness in federated learning. In *Proceedings of the 2022 ACM Conference on Fairness, Accountability, and Transparency*. 142–159. doi:10.48550/arXiv.2201.08304
- [66] Afroditi Papadaki, Natalia Martinez, Martin Bertran, Guillermo Sapiro, and Miguel Rodrigues. 2024. Federated Fairness without Access to Sensitive Groups. *arXiv preprint arXiv:2402.14929* (2024). doi:10.1007/11890348_39

- [67] Dana Pessach and Erez Shmueli. 2022. A review on fairness in machine learning. *ACM Computing Surveys (CSUR)* 55, 3 (2022), 1–44. doi:10.1145/3494672
- [68] Susanna Pirttikangas, Kaori Fujinami, and Tatsuo Nakajima. 2006. Feature selection and activity recognition from wearable sensors. In *Ubiquitous Computing Systems: Third International Symposium, UCS 2006, Seoul, Korea, October 11-13, 2006. Proceedings* 3. Springer, 516–527. doi:10.1007/11890348_39
- [69] Daniele Puccinelli and Martin Haenggi. 2005. Wireless sensor networks: applications and challenges of ubiquitous sensing. *IEEE Circuits and systems magazine* 5, 3 (2005), 19–31. doi:10.1109/MCAS.2005.1507522
- [70] Zhe Qu, Xingyu Li, Rui Duan, Yao Liu, Bo Tang, and Zhuo Lu. 2022. Generalized federated learning via sharpness aware minimization. In *International conference on machine learning*. PMLR, 18250–18280.
- [71] Vishnu V Ratnam, Hao Chen, Hao-Hsuan Chang, Abhishek Sehgal, and Jianzhong Zhang. 2024. Optimal preprocessing of WiFi CSI for sensing applications. *IEEE Transactions on Wireless Communications* 23, 9 (2024), 10820–10833. doi:10.1109/TWC.2024.3376332
- [72] Nicola Rieke, Jonny Hancox, Wenqi Li, Fausto Milletari, Holger R Roth, Shadi Albarqouni, Spyridon Bakas, Mathieu N Galtier, Bennett A Landman, Klaus Maier-Hein, et al. 2020. The future of digital health with federated learning. *NPJ digital medicine* 3, 1 (2020), 1–7. doi:10.1038/s41746-020-00323-1
- [73] Adepu Ravi Sankar, Yash Khasbage, Rahul Vigneswaran, and Vineeth N Balasubramanian. 2021. A deeper look at the hessian eigenspectrum of deep neural networks and its applications to regularization. In *Proceedings of the AAAI Conference on Artificial Intelligence*, Vol. 35. 9481–9488.
- [74] D Sathya, V Chaitra, Srividya Adiga, G Srujana, and M Priyanka. 2023. Systematic Review on on-Air Hand Doodle System for the Purpose of Authentication. In *2023 Third International Conference on Artificial Intelligence and Smart Energy (ICAIS)*. IEEE, 1460–1467. doi:10.1109/ICAIS56108.2023.10073858
- [75] Reza Shahbazian and Irina Trubitsyna. 2023. Human Sensing by using Radio Frequency Signals: A Survey on Occupancy and Activity Detection. *IEEE Access* (2023). doi:10.1109/ACCESS.2023.3269843
- [76] Thanveer Shaik, Xiaohui Tao, Niall Higgins, Raj Gururajan, Yuefeng Li, Xujuan Zhou, and U Rajendra Acharya. 2022. Fedstack: Personalized activity monitoring using stacked federated learning. *Knowledge-Based Systems* 257 (2022), 109929. doi:10.48550/arXiv.2209.13080
- [77] Harshit Sharma, Yi Xiao, Victoria Tumanova, and Asif Salekin. 2022. Psychophysiological Arousal in Young Children Who Stutter: An Interpretable AI Approach. *Proceedings of the ACM on interactive, mobile, wearable and ubiquitous technologies* 6, 3 (2022), 1–32. doi:10.1145/3550326
- [78] Sidak Pal Singh and Dan Alistarh. 2020. Woodfisher: Efficient second-order approximation for neural network compression. *Advances in Neural Information Processing Systems* 33 (2020), 18098–18109. doi:10.48550/arXiv.2004.14340
- [79] Valentin Thomas, Fabian Pedregosa, Bart Merriënboer, Pierre-Antoine Manzagol, Yoshua Bengio, and Nicolas Le Roux. 2020. On the interplay between noise and curvature and its effect on optimization and generalization. In *Proceedings of the Twenty Third International Conference on Artificial Intelligence and Statistics*. PMLR, 3503–3513. doi:10.48550/arXiv.1906.07774 ISSN: 2640-3498.
- [80] Cuong Tran. 2023. *The Interplay Between Privacy and Fairness in Learning and Decision Making Problems*. Ph. D. Dissertation. Syracuse University. <https://surface.syr.edu/etd/1764/>
- [81] Cuong Tran, Ferdinando Fioretto, Jung-Eun Kim, and Rakshit Naidu. 2022. Pruning has a disparate impact on model accuracy. *Advances in Neural Information Processing Systems* 35 (2022), 17652–17664. doi:10.48550/arXiv.2205.13574
- [82] Ben Van Werkhoven, Jason Maassen, Frank J Seinstra, and Henri E Bal. 2014. Performance models for CPU-GPU data transfers. In *2014 14th IEEE/ACM International Symposium on Cluster, Cloud and Grid Computing*. IEEE, 11–20. doi:10.1109/CCGrid.2014.16
- [83] Gideon Vos, Kelly Trinh, Zoltan Sarnyai, and Mostafa Rahimi Azghadi. 2023. Generalizable Machine Learning for Stress Monitoring from Wearable Devices: A Systematic Literature Review. *International Journal of Medical Informatics* (2023), 105026. doi:10.1016/j.ijmedinf.2023.105026
- [84] Dong Wang, Boleslaw K Szymanski, Tarek Abdelzaher, Heng Ji, and Lance Kaplan. 2019. The age of social sensing. *Computer* 52, 1 (2019), 36–45. doi:10.1109/MC.2018.2890173
- [85] Fei Wang, Jinsong Han, Shiyuan Zhang, Xu He, and Dong Huang. 2018. Csi-net: Unified human body characterization and pose recognition. *arXiv preprint arXiv:1810.03064* (2018).
- [86] Tianyu Wang, Zicheng Wang, and Jiajia Yu. 2024. Zeroth-order Low-rank Hessian Estimation via Matrix Recovery. *arXiv preprint arXiv:2402.05385* (2024). doi:10.48550/arXiv.2402.05385
- [87] Wei Wen, Yandan Wang, Feng Yan, Cong Xu, Chunpeng Wu, Yiran Chen, and Hai Li. 2018. Smoothout: Smoothing out sharp minima to improve generalization in deep learning. *arXiv preprint arXiv:1805.07898* (2018). doi:10.48550/arXiv.1805.07898
- [88] Samuel Williams, Andrew Waterman, and David Patterson. 2009. Roofline: an insightful visual performance model for multicore architectures. *Commun. ACM* 52, 4 (2009), 65–76. doi:10.1145/1498765.1498785
- [89] Chenrui Wu, Haishuai Wang, Xiang Zhang, Zhen Fang, and Jiajun Bu. 2024. Spatio-temporal Heterogeneous Federated Learning for Time Series Classification with Multi-view Orthogonal Training. In *Proceedings of the 32nd ACM International Conference on Multimedia*. 2613–2622. doi:10.1145/3664647.3680733

- [90] Yi Xiao, Harshit Sharma, Zhongyang Zhang, Dessa Bergen-Cico, Tauhidur Rahman, and Asif Salekin. 2024. Reading Between the Heat: Co-Teaching Body Thermal Signatures for Non-intrusive Stress Detection. *Proceedings of the ACM on Interactive, Mobile, Wearable and Ubiquitous Technologies* 7, 4 (2024), 1–30. doi:10.1145/3631441
- [91] Xuhai Xu, Xin Liu, Han Zhang, Weichen Wang, Subigya Nepal, Yasaman Sefidgar, Woosuk Seo, Kevin S Kuehn, Jeremy F Huckins, Margaret E Morris, et al. 2023. GLOBEM: Cross-Dataset Generalization of Longitudinal Human Behavior Modeling. *Proceedings of the ACM on Interactive, Mobile, Wearable and Ubiquitous Technologies* 6, 4 (2023), 1–34. doi:10.1145/3569485
- [92] Zikang Xu, Shang Zhao, Quan Quan, Qingsong Yao, and S Kevin Zhou. 2023. Fairadabn: Mitigating unfairness with adaptive batch normalization and its application to dermatological disease classification. In *International Conference on Medical Image Computing and Computer-Assisted Intervention*. Springer, 307–317. doi:10.48550/arXiv.2303.08325
- [93] Jianfei Yang, Xinyan Chen, Dazhuo Wang, Han Zou, Chris Xiaoxuan Lu, Sumei Sun, and Lihua Xie. 2023. SenseFi: A Library and Benchmark on Deep-Learning-Empowered WiFi Human Sensing. *Patterns* 4, 3 (2023). doi:10.48550/arXiv.2207.07859
- [94] Dezhong Yao, Ziquan Zhu, Tongtong Liu, Zhiqiang Xu, and Hai Jin. 2024. Rethinking Personalized Federated Learning from Knowledge Perspective. In *Proceedings of the 53rd International Conference on Parallel Processing*. 991–1000. doi:10.1145/3673038.367311
- [95] Sofia Yfantidou, Marios Constantinides, Dimitris Spathis, Athena Vakali, Daniele Quercia, and Fahim Kawsar. 2023. Beyond Accuracy: A Critical Review of Fairness in Machine Learning for Mobile and Wearable Computing. *arXiv preprint arXiv:2303.15585* (2023).
- [96] Sofia Yfantidou, Marios Constantinides, Dimitris Spathis, Athena Vakali, Daniele Quercia, and Fahim Kawsar. 2023. The state of algorithmic fairness in mobile human-computer interaction. In *Proceedings of the 25th International Conference on Mobile Human-Computer Interaction*. 1–7. doi:10.1145/3565066.3608685
- [97] Sofia Yfantidou, Pavlos Sermpezis, Athena Vakali, and Ricardo Baeza-Yates. 2023. Uncovering bias in personal informatics. *Proceedings of the ACM on Interactive, Mobile, Wearable and Ubiquitous Technologies* 7, 3 (2023), 1–30. doi:10.1145/3610914
- [98] Khadija Zanna and Akane Sano. 2024. Enhancing Fairness and Performance in Machine Learning Models: A Multi-Task Learning Approach with Monte-Carlo Dropout and Pareto Optimality. *arXiv preprint arXiv:2404.08230* (2024). doi:10.48550/arXiv.2404.08230
- [99] Yuchen Zeng, Hongxu Chen, and Kangwook Lee. 2021. Improving fairness via federated learning. *arXiv preprint arXiv:2110.15545* (2021). doi:10.48550/arXiv.2110.15545
- [100] Daniel Yue Zhang, Ziyi Kou, and Dong Wang. 2020. Fairfl: A fair federated learning approach to reducing demographic bias in privacy-sensitive classification models. In *2020 IEEE International Conference on Big Data (Big Data)*. IEEE, 1051–1060. doi:10.1109/BigData50022.2020.9378043
- [101] Han Zhang, Leijie Wang, Yilun Sheng, Xuhai Xu, Jennifer Mankoff, and Anind K Dey. 2023. A Framework for Designing Fair Ubiquitous Computing Systems. In *Adjunct Proceedings of the 2023 ACM International Joint Conference on Pervasive and Ubiquitous Computing & the 2023 ACM International Symposium on Wearable Computing*. 366–373. doi:10.48550/arXiv.2308.08710
- [102] He Zhang, Xingliang Yuan, and Shirui Pan. 2024. Unraveling privacy risks of individual fairness in graph neural networks. In *2024 IEEE 40th International Conference on Data Engineering (ICDE)*. IEEE, 1712–1725. doi:10.48550/arXiv.2301.12951
- [103] Tuo Zhang, Lei Gao, Sunwoo Lee, Mi Zhang, and Salman Avestimehr. 2023. TimelyFL: Heterogeneity-aware Asynchronous Federated Learning with Adaptive Partial Training. In *Proceedings of the IEEE/CVF Conference on Computer Vision and Pattern Recognition*. 5064–5073. doi:10.48550/arXiv.2304.06947
- [104] Wenbin Zhang and Eirini Ntoutsis. 2019. Faht: an adaptive fairness-aware decision tree classifier. *arXiv preprint arXiv:1907.07237* (2019). doi:10.48550/arXiv.1907.07237
- [105] Yi Zhang, Yue Zheng, Kun Qian, Guidong Zhang, Yunhao Liu, Chenshu Wu, and Zheng Yang. 2021. Widar3. 0: Zero-effort cross-domain gesture recognition with Wi-Fi. *IEEE Transactions on Pattern Analysis and Machine Intelligence* 44, 11 (2021), 8671–8688. doi:10.1145/3307334.3326081
- [106] Yue Zhao, Meng Li, Liangzhen Lai, Naveen Suda, Damon Civin, and Vikas Chandra. 2018. Federated learning with non-iid data. *arXiv preprint arXiv:1806.00582* (2018). doi:10.48550/arXiv.1806.00582
- [107] Zhi Zhou, Xu Chen, En Li, Liekang Zeng, Ke Luo, and Junshan Zhang. 2019. Edge intelligence: Paving the last mile of artificial intelligence with edge computing. *Proc. IEEE* 107, 8 (2019), 1738–1762. <https://api.semanticscholar.org/CorpusID:165163986>
- [108] Ligeng Zhu, Hongzhou Lin, Yao Lu, Yujun Lin, and Song Han. 2021. Delayed gradient averaging: Tolerate the communication latency for federated learning. *Advances in neural information processing systems* 34 (2021), 29995–30007. doi:10.5555/3540261.3542557

A Methodological Transparency & Reproducibility Appendix (META)

A.1 Dataset and Model Description

This section provides a detailed overview of the dataset and the models we utilized in our evaluations.

A.1.1 Dataset Description. WIDAR Dataset: The WIDAR3.0 dataset [105] contains WIFI channel state information (CSI) [38] which represents the variation in the Wifi channel portrayed by commodity wifi devices [38, 105]. The WIFI CSI contains fine-grained information about variations in the Wifi channel based on the Doppler phenomenon [105]. These signals have been used by prior researchers for gesture detection [105], presence detection [74], pose estimation [85], human identification and activity detection [75]. We have used it as one of the HAR (Human Activity Recognition) datasets. The dataset contains data from 16 participants, 4 Females, and 12 Males, with five different orientations (labeled as 1 to 5). We removed a female participant from the dataset due to the absence of ground truth. The selected two gestures, ‘Slide’ and ‘Sweep,’ had data in all orientations for male and female participants in the presence of the wifi sensor. Since all participants had an equal number of samples in different orientations, i.e., orientations 1 to 5, we created a disparity in the dataset based on orientations by randomly sub-sampling 50% of the data belonging to orientations 4 and 5. This was done to create a training imbalance representative of real-life scenarios where some groups have more representation compared to others. We considered labels 1 to 3 as major orientation and the rest as minor orientation. For our work, we have trained a model to perform binary classification to detect Sweep vs. Slide gestures using WIFI-CSI data and fairness on the basis of ‘sex’ and ‘orientation’ as sensitive attributes.

HuGaDB Dataset: We have also utilized the HuGaDB (Human Gait Database) dataset [12] for HAR purposes, which comprises a diverse array of human activity recordings from 18 participants. The participant group includes 4 females and 14 males. In our work, we trained a binary classification model to distinguish between Standing and other activities from this dataset, with fairness considerations based on ‘sex’ as the sensitive attribute.

Stress sensing Dataset: Xiao et al. [90] collected this dataset. This dataset was obtained from 48 individuals, including 40 females and 8 males, who participated in four different stress-inducing tasks (Arithmetic, Bad Memory, Stress Videos, Pre-condition), each associated with unique stressors. The dataset is not publicly available yet; Access to the dataset has been obtained through proper IRB approvals/extensions. Due to the continuation of data collection by the Xiao et al. [90]’s research group, this paper’s reported dataset has more individuals than reported by the Xiao et al. [90] paper. The dataset has individuals wearing Empatica E4 [59] in their left and/or right hands and individuals’ sex information. Hence, this paper utilized ‘hand’ information and ‘sex’ as sensitive attributes for evaluation. Utilizing this dataset, we performed a binary stress detection classification task.

PERCEPT-R dataset: The PERCEPT-R corpus [6] is an open-access clinical speech repository specialized for the study of American English rhotic production /ɹ/ in children and adolescents. The dataset comprises over 32 hours of citation speech (single words and short phrases) is a part of an ongoing longitudinal study collected from 281 participants aged 6 to 24 years ($\mu = 11.3$ years), including typically developing speakers and those with Residual Speech Sound Disorders (RSSD). For our evaluation, we utilize a publicly available subset of 76 participants. Audio samples were originally recorded as 16-bit PCM WAV files at 44.1 kHz. Ground-truth labels were derived from perceptual judgments by trained listeners (speech-language pathologists) or crowdsourced raters, identifying productions as either “rhotic” (correct) or “derhotic” (incorrect). Feature extraction focused on spectral characteristics critical for rhoticity, specifically the distance between the second and third formants (F3-F2), which serves as a primary acoustic marker for /ɹ/ quality in American English. Consistent with the dataset’s clinical demographics, sex is retained as a sensitive attribute due to the higher prevalence of RSSD in males compared to females which was also reflected in the dataset distribution with 50 male and 26 female participant.

A.1.2 Model Description. **WIDAR Model:** The WIDAR Model architecture (adapted from [93]) is comprised of two fully connected layers within a sequential module, featuring an input size of $22 * 20 * 20$. A dropout layer with a 40% dropout rate and a Rectified Linear Unit (ReLU) activation function follow the first linear layer, while the second linear layer outputs the classification result. The model reshapes the input tensor during the forward pass and incorporates dropout layers to mitigate over-fitting.

HugaDB Model: The HugaDB model architecture (adapted from [68]) is characterized by its complexity, featuring two sequential fully connected layers. The first layer consists of linear transformations with input and output sizes of 792 to 1024, followed by dropout with a 30% probability, Rectified Linear Unit (ReLU) activation, and Instance Normalization. Subsequently, another linear layer reduces the dimensionality to 512, followed by similar dropout, ReLU, and Instance Normalization. The second layer further reduces the dimensionality from 512 to 128, followed by a linear layer with an output size equal to the specified number of classes. The final output is obtained by applying the sigmoid function to the result. During the forward pass, the input tensor is processed through these layers, reshaped when necessary, and the output is returned after applying the sigmoid function.

Stress sensing Model: The Stress sensing model architecture (adapted from [77]) comprises three sequential fully connected layers. The first layer takes input of size 34 and produces an output of size 64, incorporating batch normalization and Rectified Linear Unit (ReLU) activation. The second layer further processes the output, reducing it to size 128 with ReLU activation. The final layer transforms the output to the specified embedding size.

Percept-R model: The Percept-R model utilizes a compact 1D Convolutional Neural Network (CNN) designed to classify multivariate time-series data. The input consists of 5 acoustic feature channels over a sequence length of 60 time steps.

The feature extraction block is composed of two consecutive 1D convolutional layers. The first layer maps the 5 input channels to 3 output channels using a kernel size of 5 and a stride of 1. The second layer reduces the dimensionality further, mapping the 3 channels to a single channel, maintaining a kernel size of 5 and a stride of 1. This process results in a feature map of length 52, which is subsequently flattened.

The classification head is a MLP consisting of two hidden layers, each containing 32 units with Hardswish activation functions. The final layer is a linear projection mapping the 32 latent features to 2 output units for binary classification.

A.1.3 Client Distribution: This section describes the client distribution splits used to address **RQ-1** (Table 3) and **RQ-2** (Table 4) in the main text. The distribution of multi-person clients is reported in Table 11 (a), while Table 11 (b) summarizes the distribution of both single- and multi-person clients.

WIDAR		
Client	Male	Female
Client 1	4	1
Client 2	4	1
Client 3	4	1

HugaDB		
Client	Male	Female
Client 1	4	1
Client 2	4	1
Client 3	4	1
Client 4	2	1

Stress Sensing		
Client	Male	Female
Client 1	2	4
Client 2	4	2
Client 3	1	6
Client 4	1	6
Client 5	2	3
Client 6	1	7
Client 7	3	6

PERCEPT-R		
Client	Male	Female
Client 0	4	0
Client 1	4	1
Client 2	2	3
Client 3	4	1
Client 4	3	2
Client 5	3	2
Client 6	1	3
Client 7	1	1
Client 8	0	3
Client 9	3	0
Client 10	3	0
Client 11	4	1
Client 12	1	1
Client 13	4	1
Client 14	1	3
Client 15	1	1
Client 16	1	1
Client 17	3	0
Client 18	2	0
Client 19	1	1
Client 20	2	0
Client 21	2	1

WIDAR		
Client	Male	Female
Client 1	1	1
Client 2	2	1
Client 3	1	0
Client 4	2	0
Client 5	2	1
Client 6	1	0
Client 7	1	0
Client 8	2	0

HugaDB		
Client	Male	Female
Client 1	6	0
Client 2	5	1
Client 3	0	2
Client 4	0	1

Stress Sensing		
Client	Male	Female
Client 1	1	0
Client 2	3	0
Client 3	6	10
Client 4	0	6
Client 5	3	7
Client 6	2	9
Client 7	0	1

PERCEPT-R		
Client	Male	Female
Client 0	2	2
Client 1	1	1
Client 2	3	2
Client 3	3	1
Client 4	3	0
Client 5	3	1
Client 6	2	0
Client 7	1	1
Client 8	2	3
Client 9	1	0
Client 10	1	0
Client 11	1	0
Client 12	2	1
Client 13	3	1
Client 14	3	2
Client 15	2	2
Client 16	3	0
Client 17	3	0
Client 18	2	2
Client 19	3	0
Client 20	1	2
Client 21	1	1
Client 22	2	1
Client 23	0	1
Client 24	1	1
Client 25	1	1
Client 26	0	2
Client 27	1	0
Client 28	1	0

(a) Multi-person Clients

(b) Single & Multi-person Clients

Table 11. Client distribution across WIDAR, HugaDB, Stress sensing and Percept-R Datasets for (a) Multi-person clients and (b) Single and Multi-person clients

A.1.4 Reproducibility of Results. We conducted experiments using three different random seeds, with each configuration evaluated via 5-fold cross-validation. For clarity, we report representative results from a single seed in the main text. The complete results for the remaining two seeds are provided in supplementary tables: Table 12 corresponds to **RQ-1**, Table 13 reports results for **RQ-2** and **RQ-3**, and Table 14 presents the results for **RQ-4**.

Dataset	Model	Mean F1 Score \pm std (\uparrow)	Mean EO Gap \pm std (\downarrow)	Mean FATE Score $\times 10^{-1}$ (\uparrow)	Seed	
WIDAR	FedAvg	0.862 \pm 0.0014	0.410 \pm 0.0151	0.0000	123	
	FedSAM	0.849 \pm 0.0066	0.397 \pm 0.0204	0.14	123	
	FedSWA	0.858 \pm 0.0009	0.403 \pm 0.0119	0.10	123	
	FedSRCVAR	0.728 \pm 0.0407	0.343 \pm 0.0521	0.05	123	
	KD-FedAvg	0.847 \pm 0.0016	0.400 \pm 0.0018	0.03	123	
	CurvFed	0.767 \pm 0.0383	0.352 \pm 0.0121	0.29	123	
	FedAvg	0.862 \pm 0.0006	0.412 \pm 0.0154	0.0000	12345	
	FedSAM	0.860 \pm 0.0044	0.407 \pm 0.0182	0.10	12345	
	FedSWA	0.859 \pm 0.0030	0.405 \pm 0.0142	0.15	12345	
	FedSRCVAR	0.725 \pm 0.0187	0.345 \pm 0.0534	0.02	12345	
	KD-FedAvg	0.849 \pm 0.0123	0.392 \pm 0.0299	0.33	12345	
	CurvFed	0.769 \pm 0.0466	0.336 \pm 0.0284	0.77	12345	
	Stress sensing	FedAvg	0.790 \pm 0.0041	0.335 \pm 0.0324	0.0000	123
		FedSAM	0.800 \pm 0.0139	0.321 \pm 0.0001	0.56	123
FedSWA		0.744 \pm 0.0096	0.294 \pm 0.0014	0.65	123	
FedSRCVAR		0.695 \pm 0.0153	0.241 \pm 0.0154	1.61	123	
KD-FedAvg		0.718 \pm 0.0254	0.248 \pm 0.0045	1.70	123	
CurvFed		0.793 \pm 0.0077	0.254 \pm 0.0065	2.46	123	
FedAvg		0.751 \pm 0.0331	0.351 \pm 0.0412	0.0000	12345	
FedSAM		0.779 \pm 0.0114	0.334 \pm 0.0232	0.84	12345	
FedSWA		0.764 \pm 0.0084	0.314 \pm 0.0021	1.23	12345	
FedSRCVAR		0.675 \pm 0.0183	0.258 \pm 0.0112	1.62	12345	
KD-FedAvg		0.773 \pm 0.0087	0.278 \pm 0.0097	2.39	12345	
CurvFed		0.793 \pm 0.0065	0.261 \pm 0.0007	3.12	12345	
HugaDB		FedAvg	0.852 \pm 0.0253	0.478 \pm 0.0446	0.0000	123
		FedSAM	0.787 \pm 0.0178	0.438 \pm 0.0036	0.07	123
	FedSWA	0.827 \pm 0.0090	0.439 \pm 0.0138	0.53	123	
	FedSRCVAR	0.854 \pm 0.0176	0.410 \pm 0.0097	1.45	123	
	KD-FedAvg	0.762 \pm 0.0132	0.424 \pm 0.0154	0.08	123	
	CurvFed	0.880 \pm 0.0129	0.406 \pm 0.0037	1.84	123	
	FedAvg	0.862 \pm 0.0088	0.488 \pm 0.0264	0.0000	12345	
	FedSAM	0.789 \pm 0.0068	0.368 \pm 0.1589	0.09	12345	
	FedSWA	0.825 \pm 0.0365	0.379 \pm 0.1325	0.23	12345	
	FedSRCVAR	0.857 \pm 0.0123	0.390 \pm 0.0425	0.34	12345	
	KD-FedAvg	0.796 \pm 0.0461	0.374 \pm 0.1653	0.01	12345	
	CurvFed	0.892 \pm 0.0072	0.406 \pm 0.0037	0.34	12345	
	PERCEPT-R	FedAvg	0.778 \pm 0.0051	0.131 \pm 0.0126	0.000	42
		FedSAM	0.773 \pm 0.0059	0.132 \pm 0.0173	-0.11	42
FedSWA		0.777 \pm 0.0049	0.131 \pm 0.0171	-0.02	42	
FedSRCVAR		0.774 \pm 0.0053	0.126 \pm 0.0238	0.30	42	
KD-FedAvg		0.772 \pm 0.0053	0.124 \pm 0.0189	0.45	42	
CurvFed		0.775 \pm 0.0073	0.112 \pm 0.0142	1.36	42	
FedAvg		0.782 \pm 0.0029	0.134 \pm 0.0178	0.000	123	
FedSAM		0.779 \pm 0.0040	0.133 \pm 0.0110	0.08	123	
FedSWA		0.790 \pm 0.0061	0.136 \pm 0.0118	-0.66	123	
FedSRCVAR		0.776 \pm 0.0034	0.130 \pm 0.0154	0.25	123	
KD-FedAvg		0.779 \pm 0.0034	0.153 \pm 0.0170	-1.40	123	
CurvFed		0.769 \pm 0.0068	0.116 \pm 0.0103	1.20	123	

Table 12. Performance metrics for federated learning models evaluated (corresponding to **RQ-1**) with different random seeds and 5-fold cross-validation across datasets. Metrics with \uparrow indicate higher is better, while metrics with \downarrow indicate lower is better. *Note: While some methods perform better on individual F1 or EO Gap metrics, CurvFed attains the highest FATE score, reflecting the overall fairness-utility balance*

Dataset	Client	Model	F1 Score	EO Gap	FATE $\times 10^{-1}$	Seed	Dataset	Client	Model	F1 Score	EO Gap	FATE $\times 10^{-1}$	Seed
			Mean \pm Std (\uparrow)	Mean \pm Std (\downarrow)	Mean (\uparrow)					Mean \pm Std (\downarrow)	Mean (\uparrow)		
WIDAR	Single & Multi Person	FedAvg	0.836 \pm 0.0165	0.435 \pm 0.0114	0.000	123	HugaDB	Single & Multi Person	FedAvg	0.863 \pm 0.0136	0.454 \pm 0.0019	0.000	123
		FedSAM	0.822 \pm 0.0143	0.411 \pm 0.0032	0.375	123			FedSAM	0.869 \pm 0.0152	0.419 \pm 0.0021	0.848	123
		FedSWA	0.842 \pm 0.0323	0.442 \pm 0.0034	-0.087	123			FedSWA	0.860 \pm 0.0065	0.454 \pm 0.0042	-0.027	123
		FedSRCVaR	0.716 \pm 0.0286	0.391 \pm 0.0042	-0.423	123			KD-FedAvg	0.763 \pm 0.0124	0.400 \pm 0.0031	0.047	123
		KD-FedAvg	0.797 \pm 0.0023	0.398 \pm 0.0032	0.391	123			FedSRCVaR	0.807 \pm 0.0092	0.384 \pm 0.0057	0.902	123
		CurvFed	0.793 \pm 0.0089	0.379 \pm 0.0089	0.772	123			CurvFed	0.816 \pm 0.0098	0.385 \pm 0.0013	0.980	123
		FedAvg	0.841 \pm 0.0189	0.431 \pm 0.0072	0.000	12345			FedAvg	0.863 \pm 0.0231	0.441 \pm 0.0042	0.000	12345
		FedSAM	0.835 \pm 0.0102	0.422 \pm 0.0116	0.149	12345			FedSAM	0.848 \pm 0.0281	0.413 \pm 0.0053	0.544	12345
		FedSWA	0.853 \pm 0.0108	0.422 \pm 0.0113	0.359	12345			FedSWA	0.850 \pm 0.0192	0.421 \pm 0.0093	0.381	12345
		FedSRCVaR	0.725 \pm 0.0098	0.412 \pm 0.0092	-0.926	12345			KD-FedAvg	0.781 \pm 0.0189	0.419 \pm 0.0047	-0.365	12345
		KD-FedAvg	0.794 \pm 0.0086	0.393 \pm 0.0153	0.309	12345			FedSRCVaR	0.832 \pm 0.0192	0.413 \pm 0.0144	0.345	12345
		CurvFed	0.791 \pm 0.0057	0.373 \pm 0.0087	0.763	12345			CurvFed	0.812 \pm 0.0095	0.393 \pm 0.0186	0.571	12345
	Single Person Only	FedAvg	0.851 \pm 0.0095	0.452 \pm 0.0132	0.000	123		FedAvg	0.882 \pm 0.0139	0.463 \pm 0.0049	0.000	123	
		FedSAM	0.842 \pm 0.0187	0.431 \pm 0.0134	0.355	123		FedSAM	0.876 \pm 0.0052	0.451 \pm 0.0182	0.196	123	
		FedSWA	0.856 \pm 0.0039	0.434 \pm 0.0049	0.449	123		FedSWA	0.883 \pm 0.0231	0.442 \pm 0.0086	0.480	123	
		FedSRCVaR	0.712 \pm 0.0243	0.412 \pm 0.0096	-0.764	123		FedSRCVaR	0.805 \pm 0.0163	0.412 \pm 0.0212	0.237	123	
		KD-FedAvg	0.782 \pm 0.0096	0.410 \pm 0.0172	0.122	123		KD-FedAvg	0.789 \pm 0.0124	0.401 \pm 0.0089	0.287	123	
		CurvFed	0.794 \pm 0.0229	0.392 \pm 0.0059	0.650	123		CurvFed	0.831 \pm 0.0112	0.402 \pm 0.0125	0.761	123	
		FedAvg	0.857 \pm 0.0113	0.431 \pm 0.0098	0.000	12345		FedAvg	0.873 \pm 0.0239	0.456 \pm 0.0134	0.000	12345	
		FedSAM	0.842 \pm 0.0142	0.420 \pm 0.0078	0.093	12345		FedSAM	0.864 \pm 0.0125	0.452 \pm 0.0214	-0.018	12345	
		FedSWA	0.852 \pm 0.0038	0.424 \pm 0.0042	0.126	12345		FedSWA	0.795 \pm 0.0093	0.406 \pm 0.0094	0.196	12345	
		FedSRCVaR	0.723 \pm 0.0241	0.370 \pm 0.0049	-0.143	12345		FedSRCVaR	0.794 \pm 0.0086	0.411 \pm 0.0002	0.088	12345	
		KD-FedAvg	0.782 \pm 0.0173	0.403 \pm 0.0020	-0.223	12345		KD-FedAvg	0.773 \pm 0.0179	0.398 \pm 0.0041	0.136	12345	
		CurvFed	0.788 \pm 0.0084	0.389 \pm 0.0043	0.180	12345		CurvFed	0.832 \pm 0.0107	0.401 \pm 0.0085	0.746	12345	
Stress Sensing	Single & Multi Person	FedAvg	0.771 \pm 0.0129	0.394 \pm 0.0188	0.000	123	PERCEPT-R	Single & Multi Person	FedAvg	0.778 \pm 0.0068	0.114 \pm 0.0130	0.000	42
		FedSAM	0.749 \pm 0.0058	0.382 \pm 0.0123	0.020	123			FedSAM	0.781 \pm 0.0067	0.109 \pm 0.0106	0.43	42
		FedSWA	0.843 \pm 0.0151	0.317 \pm 0.0096	2.904	123			FedSWA	0.781 \pm 0.0051	0.113 \pm 0.0115	0.09	42
		KD-FedAvg	0.760 \pm 0.0192	0.288 \pm 0.0092	2.534	123			FedSRCVaR	0.784 \pm 0.0050	0.111 \pm 0.0072	0.37	42
		FedSRCVaR	0.719 \pm 0.0091	0.294 \pm 0.0146	1.858	123			KD-FedAvg	0.779 \pm 0.0078	0.114 \pm 0.0106	0.003	42
		CurvFed	0.864 \pm 0.0098	0.265 \pm 0.0129	4.477	123			CurvFed	0.775 \pm 0.0056	0.103 \pm 0.0107	0.96	42
		FedAvg	0.761 \pm 0.0203	0.361 \pm 0.0084	0.000	12345			FedAvg	0.782 \pm 0.0063	0.122 \pm 0.0169	0.000	123
		FedSAM	0.769 \pm 0.0142	0.382 \pm 0.0130	-0.476	12345			FedSAM	0.779 \pm 0.0044	0.114 \pm 0.0197	0.62	123
		FedSWA	0.782 \pm 0.0123	0.350 \pm 0.0145	0.596	12345			FedSWA	0.780 \pm 0.0043	0.113 \pm 0.0221	0.73	123
		KD-FedAvg	0.705 \pm 0.0094	0.282 \pm 0.0134	1.448	12345			FedSRCVaR	0.786 \pm 0.0059	0.122 \pm 0.0154	0.05	123
		FedSRCVaR	0.721 \pm 0.0078	0.274 \pm 0.0198	1.887	12345			KD-FedAvg	0.782 \pm 0.0056	0.127 \pm 0.0173	-0.37	123
		CurvFed	0.812 \pm 0.0099	0.262 \pm 0.0199	3.406	12345			CurvFed	0.780 \pm 0.0106	0.110 \pm 0.0138	0.93	123
	Single Person Only	FedAvg	0.771 \pm 0.0039	0.391 \pm 0.0057	0.000	123		FedAvg	0.772 \pm 0.0039	0.105 \pm 0.0067	0.000	42	
		FedSAM	0.768 \pm 0.0152	0.358 \pm 0.0183	0.798	123		FedSAM	0.770 \pm 0.0039	0.103 \pm 0.0159	0.15	42	
		FedSWA	0.754 \pm 0.0092	0.382 \pm 0.0126	0.008	123		FedSWA	0.766 \pm 0.0038	0.101 \pm 0.0152	0.25	42	
		FedSRCVaR	0.686 \pm 0.0115	0.224 \pm 0.0138	3.159	123		FedSRCVaR	0.768 \pm 0.0047	0.105 \pm 0.0078	-0.09	42	
		KD-FedAvg	0.685 \pm 0.0115	0.262 \pm 0.0172	2.181	123		KD-FedAvg	0.772 \pm 0.0043	0.104 \pm 0.0057	0.04	42	
		CurvFed	0.743 \pm 0.0093	0.233 \pm 0.0191	3.689	123		CurvFed	0.768 \pm 0.0106	0.077 \pm 0.0191	2.66	42	
		FedAvg	0.764 \pm 0.0083	0.382 \pm 0.0083	0.000	12345		FedAvg	0.766 \pm 0.0093	0.105 \pm 0.0165	0.000	123	
		FedSAM	0.752 \pm 0.0091	0.378 \pm 0.0073	-0.032	12345		FedSAM	0.771 \pm 0.0033	0.105 \pm 0.0066	0.09	123	
		FedSWA	0.759 \pm 0.0173	0.361 \pm 0.0042	0.510	12345		FedSWA	0.769 \pm 0.0037	0.110 \pm 0.0075	-0.40	123	
		FedSRCVaR	0.673 \pm 0.0292	0.229 \pm 0.0183	2.850	12345		FedSRCVaR	0.766 \pm 0.0058	0.103 \pm 0.0144	0.22	123	
		KD-FedAvg	0.700 \pm 0.0093	0.263 \pm 0.0129	2.294	12345		KD-FedAvg	0.769 \pm 0.0062	0.109 \pm 0.0088	-0.32	123	
		CurvFed	0.742 \pm 0.0040	0.255 \pm 0.0042	3.058	12345		CurvFed	0.751 \pm 0.0050	0.068 \pm 0.0163	3.33	123	

Table 13. Performance metrics for all datasets evaluated across different client compositions (corresponding to **RQ-2**, **RQ-3**) and random seeds (5-fold cross-validation). Metrics with \uparrow indicate higher is better, while \downarrow indicates lower is better. *Note: CurvFed consistently achieves the highest FATE score.*

B Runtime benchmarking vs baseline approaches

To complement the real-world study, we benchmarked *CurvFed* against standard FL baselines (FedAvg, FedSAM) on *seven* deployment platforms—from high-performance GPUs (NVIDIA RTX 4090) to resource-constrained devices (Raspberry Pi 5, Pixel 6) to assess real-world feasibility. Across five runs using the WIDAR dataset, we measured training time, memory usage, resource utilization, and inference time on average. As shown in Table 15, *CurvFed* incurs moderate training overhead due to the Fisher penalty, similar to FedSAM’s cost for sharpness-aware updates. However, this overhead is practical—even on edge devices—and does not affect inference time.

EDA-Hand					WIDAR-Orientation				
Model	EO Gap Mean \pm Std (\downarrow)	F1 Score Mean \pm Std (\uparrow)	FATE $\times 10^{-1}$ Mean (\uparrow)	Seed	Model	EO Gap Mean \pm Std (\downarrow)	F1 Score Mean \pm Std (\uparrow)	FATE $\times 10^{-1}$ Mean (\uparrow)	Seed
FedAvg	0.453 \pm 0.0141	0.774 \pm 0.0098	0.00	123	FedAvg	0.492 \pm 0.0098	0.848 \pm 0.0015	0.00	123
FedSAM	0.443 \pm 0.0183	0.795 \pm 0.0164	0.48	123	FedSAM	0.478 \pm 0.0141	0.833 \pm 0.0195	0.11	123
FedSWA	0.451 \pm 0.0094	0.740 \pm 0.0006	-0.40	123	FedSWA	0.508 \pm 0.0472	0.878 \pm 0.0045	0.03	123
FedSRCVaR	0.389 \pm 0.0141	0.645 \pm 0.0153	-0.27	123	FedSRCVaR	0.433 \pm 0.0579	0.747 \pm 0.0115	0.01	123
KD	0.393 \pm 0.0139	0.735 \pm 0.0027	0.83	123	KD	0.443 \pm 0.0332	0.846 \pm 0.0123	0.96	123
CurvFed	0.430 \pm 0.0052	0.805 \pm 0.0019	0.90	123	CurvFed	0.374 \pm 0.0605	0.805 \pm 0.0481	1.89	123
FedAvg	0.476 \pm 0.0094	0.754 \pm 0.0067	0.00	12345	FedAvg	0.513 \pm 0.0021	0.860 \pm 0.0028	0.00	12345
FedSAM	0.476 \pm 0.0077	0.775 \pm 0.0012	0.28	12345	FedSAM	0.465 \pm 0.0168	0.844 \pm 0.0146	0.76	12345
FedSWA	0.446 \pm 0.0024	0.745 \pm 0.0169	0.50	12345	FedSWA	0.492 \pm 0.0002	0.833 \pm 0.0069	0.09	12345
FedSRCVaR	0.391 \pm 0.0211	0.695 \pm 0.0163	0.99	12345	FedSRCVaR	0.427 \pm 0.0660	0.729 \pm 0.0102	0.17	12345
KD	0.417 \pm 0.0192	0.718 \pm 0.0154	0.75	12345	KD	0.469 \pm 0.0369	0.858 \pm 0.0010	0.85	12345
CurvFed	0.423 \pm 0.0023	0.789 \pm 0.0088	1.57	12345	CurvFed	0.384 \pm 0.0085	0.812 \pm 0.0056	1.96	12345

Table 14. Multiple seed Fairness–efficacy balance under different sensitive attributes for RQ-4. Results are averaged over 5-fold cross-validation. Lower EO indicates improved fairness, while higher F1 and FATE scores reflect a better balance between predictive performance and fairness. CurvFed consistently achieves the highest FATE score.

Methods like FedSWA and FedSRCVaR were excluded as their client-side costs mirror FedAvg, with additional computations handled server-side. Overall, **CurvFed** demonstrates efficiency and feasibility across heterogeneous edge devices.

Platform	Approach	Train (s)	RSS (MBs)	Infer (s)	Train Usage (%)
Intel i9-9900K Processor	Fedavg	1.67	1074.05	0.03	48.12
	FedSAM	5.78	1147.54	0.02	48.07
	CurvFed	9.34	1287.87	0.02	48.134
AMD Ryzen 9 7950X 16-Core Processor	Fedavg	0.77	1033.62	0.01	24.93
	FedSAM	3.23	1109.04	0.01	24.30
	CurvFed	5.42	1420.88	0.01	24.52
Apple M1	Fedavg	4.02	418.916	0.16	1.05
	FedSAM	8.95	450.31	0.16	1.06
	CurvFed	11.53	387.36	0.16	1.00
Quadro RTX 5000	Fedavg	0.73	961.77	0.01	46.4
	FedSAM	0.81	1070.73	0.01	73.0
	CurvFed	1.04	1176.54	0.01	62.3
NVIDIA GeForce RTX 4090	Fedavg	0.14	954.52	0.01	15.0
	FedSAM	0.18	1063	0.01	49.1
	CurvFed	0.32	1290.88	0.01	48.6
Google Pixel 6	Fedavg	4.24	370.84	0.12	49.11
	FedSAM	13.39	337.40	0.12	49.11
	CurvFed	26.59	326.28	0.20	49.07
Raspberry Pi 5	Fedavg	13.5	518.88	0.21	48.79
	FedSAM	40.8	489	0.23	48.7
	CurvFed	56.4	490	0.22	49

Table 15. Training Time (s), Training Process (RSS) Memory Usage (MBs), Inference Time (s), Training Resource usage (%) averaged for *five* runs for FL Approaches across Different Platforms

B.0.1 Resource Utilization and Overhead Breakdown. We measured the per-batch average training time and Fisher top-eigenvalue computation time (averaged over five runs) across all our evaluation platforms using a single client from the WIDAR dataset. Results are summarized in Table 16. While Fisher computation

introduces additional cost (typically $\sim 30\text{--}40\%$ of per-batch training time), the absolute time per call remains modest (milliseconds on GPUs and tens to hundreds of milliseconds on CPUs and mobile devices). These measurements indicate that Fisher overhead scales proportionally with device compute capability and remains practical within the constraints of on-device FL training.

Platform	Avg. Train Time / batch (s)	Avg. Fisher Time / batch (s)
GPU: Quadro RTX 5000	0.027	0.010
GPU: NVIDIA RTX 4090	0.003	0.001
CPU: AMD Ryzen 9 7950X	0.076	0.029
Apple M1	0.298	0.137
Pixel 6: Cortex-A55	0.355	0.146
CPU: Intel i9-9900K	0.169	0.062
CPU: Intel i5-14600T	0.268	0.175
Jetson Nano: Cortex-A57	1.040	0.393
Raspberry Pi: Cortex-A76	1.621	0.733

Table 16. Average per-batch training time and Fisher computation time across platforms.

To contextualize these results, we also benchmarked the upload and download latency for a trained model (~ 34.4 MB) across CPU-based platforms, using Google Cloud APIs with PyDrive authentication (Table 17). Communication latency per round is on the order of *seconds*, which is *one to two orders of magnitude higher than the Fisher computation overhead per batch*. Since such communication is repeated across many FL rounds (e.g., 80 rounds for WIDAR), network transfer typically dominates the end-to-end runtime [43].

Platform	File Size (MB)	Upload (s)	Download (s)
CPU: AMD Ryzen 9 7950X	34.39	2.30	6.42
Jetson Nano: Cortex-A57	34.39	2.83	4.43
Raspberry Pi: Cortex-A76	34.39	2.42	3.96
CPU: Intel i5-14600T	34.39	3.32	3.80
Pixel 6: Cortex-A55	34.39	5.05	4.73
CPU: Intel i9-9900K	34.39	2.36	5.41

Table 17. Upload and download latency for a trained model (~ 34.4 MB) across CPU platforms.

These experiments suggest that while Fisher computation contributes a consistent overhead during local training, communication latency remains the dominant factor in federated learning deployments [43, 108]. This indicates that curvature-based regularization is computationally feasible in practice [40], with networking emerging as the primary bottleneck. Exploring lighter curvature proxies [86] and adaptive scheduling [103] remains a valuable direction for further improving scalability.

C Experiment Details

C.1 Ablation Study on Additional Datasets

We conducted a comprehensive ablation study to meticulously guide the choices in our proposed approach. The study consistently demonstrates the effectiveness of our model across all datasets. This section presents the results for the Stress sensing, HugaDB and the WIDAR dataset in Table 18. The results for PERCEPT-R were reported in the main text under Section 6.3

#	Dataset	Client-Side Training	Aggregation Strategy	F1 Score (↑)	EO Gap (↓)	FATE Score $\times 10^{-1}$ (↑)
1	WIDAR	Benign	FedAvg	0.8507	0.4263	0
2		SAM	FedAvg	0.8005	0.4251	-0.560
3		SAM	FedSWA	0.8405	0.4071	0.331
4		SAM + Eq. 11	FedSWA	0.8459	0.4058	0.424
5		(Eq11)	FedAvg	0.8253	0.3994	0.332
6		(Eq11)	W^r (Eq12)	0.8344	0.4135	0.109
7		SAM + Eq. 11	W^r (Eq12)	0.8707	0.4199	0.386
8		(Eq11)	Sharpness-Aware Aggregation	0.8409	0.3982	0.545
9		SAM	FedSWA + S(L) (Eq12* partial)	0.8737	0.4199	0.420
10		SAM	FedSWA + S(T) (Eq12* partial)	0.8590	0.4084	0.518
11		SAM	Sharpness-Aware Aggregation	0.8668	0.4161	0.429
12		SAM + Eq. 11	Sharpness-Aware Aggregation	0.8100	0.3533	1.233
13	Stress Sensing	Benign	FedAvg	0.7253	0.3069	0
14		SAM	FedAvg	0.7758	0.3034	0.812
15		SAM	FedSWA	0.7406	0.3015	0.384
16		SAM + Eq. 11	FedSWA	0.7346	0.2768	1.105
17		(Eq. 11)	FedAvg	0.7372	0.2998	0.395
18		(Eq. 11)	W^r (Eq12)	0.7345	0.2839	0.874
19		SAM + Eq. 11	W^r (Eq12)	0.8193	0.2927	1.756
20		(Eq. 11)	Sharpness-Aware Aggregation	0.7077	0.2380	1.999
21		SAM	FedSWA + S(L) (Eq12* partial)	0.8091	0.2680	2.240
22		SAM	FedSWA + S(T) (Eq12* partial)	0.7995	0.2627	2.460
23		SAM	Sharpness-Aware Aggregation	0.8224	0.2710	2.507
24		SAM + Eq. 11	Sharpness-Aware Aggregation	0.7814	0.2522	2.555
25	HugaDB	Benign	FedAvg	0.8496	0.4369	0
26		SAM	FedAvg	0.8555	0.4255	0.329
27		SAM	FedSWA	0.8418	0.4242	0.192
28		SAM + Eq. 11	FedSWA	0.8170	0.4142	0.135
29		(Eq. 11)	FedAvg	0.8567	0.4142	0.602
30		(Eq. 11)	W^r (Eq12)	0.8574	0.4083	0.746
31		SAM + Eq. 11	W^r (Eq12)	0.9016	0.4154	1.103
32		(Eq. 11)	Sharpness-Aware Aggregation	0.8510	0.4333	0.098
33		SAM	FedSWA + S(L) (Eq12* partial)	0.8934	0.4130	1.059
34		SAM	FedSWA + S(T) (Eq12* partial)	0.8888	0.4142	0.878
35		SAM	Sharpness-Aware Aggregation	0.8911	0.4095	1.110
36		SAM + Eq. 11	Sharpness-Aware Aggregation	0.8855	0.3952	1.376

Table 18. Ablation of **CurvFed**'s design choices on the WIDAR, Stress Sensing, and HugaDB datasets. **Client-Side Training** denotes the optimization or regularization applied locally at each client, while **Aggregation Strategy** specifies the server-side model aggregation rule. Unless explicitly stated, each configuration applies *only* the listed component, with no additional modifications. Metrics with \uparrow indicate higher is better, while \downarrow indicates lower is better.

We begin by establishing benign baselines using standard FedAvg aggregation without fairness-aware training (Rows 1, 13, and 25). Across datasets, these configurations achieve competitive F1 scores (0.8507 on WIDAR, 0.7253 on Stress Sensing, and 0.8496 on HugaDB) but are consistently associated with relatively high EO Gaps

(0.4263, 0.3069, and 0.4369, respectively), highlighting the presence of fairness concerns under standard federated optimization.

Introducing SAM under FedAvg aggregation (Rows 2, 14, and 26) generally improves or maintains accuracy, most notably on Stress Sensing (F1 = 0.7758, Row 14), but yields only marginal changes in EO Gap. Replacing FedAvg with FedSWA while retaining SAM (Rows 3, 15, and 27) produces mixed effects, with modest reductions in EO Gap on WIDAR and Stress Sensing, but limited improvements on HugaDB, indicating that smoother aggregation alone is insufficient to consistently address bias.

We next examine the effect of enforcing curvature-aware local training without SAM. Applying the FIM-based regularization during client-side training with FedAvg aggregation (Rows 5, 17, and 29) consistently lowers EO Gap compared to the benign baselines, while also reducing F1 scores. Replacing FedAvg with curvature-aware weighting W' (Rows 6, 18, and 30) further modifies this trade-off, sometimes improving EO Gap (e.g., Row 18 on Stress Sensing) while slightly increasing F1 score relative to FedAvg-based curvature regularization. These results indicate that restricting local optimization to flatter regions promotes fairness, albeit at the cost of predictive performance when applied in isolation.

Combining SAM with curvature-aware local training and weighted aggregation (Rows 7, 19, and 31) shifts the balance toward higher accuracy. In particular, these configurations achieve some of the highest F1 scores across datasets, including the maximum F1 on HugaDB (0.9016, Row 31). However, EO Gaps remain relatively high in these settings, suggesting that SAM-driven optimization can counteract some fairness gains introduced by curvature regularization.

We then analyze aggregation-centric interventions. Applying sharpness-aware aggregation without SAM or curvature-aware local training (Rows 8, 20, and 32) yields noticeable reductions in EO Gap across datasets, most prominently on Stress Sensing (EO Gap = 0.2380, Row 20), but often with a reduction in F1 score. Partial sharpness-aware aggregation strategies under SAM, which prioritize either predictive uncertainty or classification loss (Rows 9–10, 21–22, and 33–34), achieve strong F1 scores—such as the highest F1 on WIDAR (0.8737, Row 9)—but do not consistently minimize EO Gap.

Employing the full sharpness-aware aggregation under SAM (Rows 11, 23, and 35) provides a more balanced outcome, achieving competitive F1 scores alongside moderate EO Gaps across all datasets. These results indicate that aggregation strategies that explicitly account for both loss and curvature information can mitigate bias more effectively than partial criteria.

Finally, the full **CurvFed** configuration—integrating curvature-aware client-side training with sharpness-aware aggregation—consistently achieves the most favorable fairness–utility trade-off. On WIDAR (Row 12), this configuration yields the lowest EO Gap (0.3533) and the highest FATE score (1.233). On Stress Sensing (Row 24), it achieves an EO Gap of 0.2522 with the highest FATE score (2.555). Similarly, on HugaDB (Row 36), it attains the lowest EO Gap (0.3952) and the highest FATE score (1.376), while maintaining a strong F1 score (0.8855). Although higher absolute F1 scores are observed in some partial configurations (e.g., Row 31), the full **CurvFed** model consistently offers the most balanced performance across datasets.